Electronic Supplementary Material (ESI) for Dalton Transactions
This journal is © The Royal Society of Chemistry 2018

# Supplementary Information For:

## Extraordinary Sensitivity for $H_2S$ and Fe(III) Sensing in Aqueous Medium by Al-MIL-53-$N_3$ Metal-Organic Framework: In Vitro and In Vivo Applications of $H_2S$ Sensing

*Aniruddha Das,*[a] *Sooram Banesh,*[b] *Vishal Trivedi,* [b] *and Shyam Biswas**[a]

[a] Department of Chemistry, Indian Institute of Technology Guwahati, Guwahati, 781039 Assam, India

[b] Malaria Research Group, Department of Biosciences and Bioengineering, Indian Institute of Technology Guwahati, 781039 Assam, India

* To whom correspondence should be addressed. E-mail: sbiswas@iitg.ernet.in; Tel: 91-3612583309.

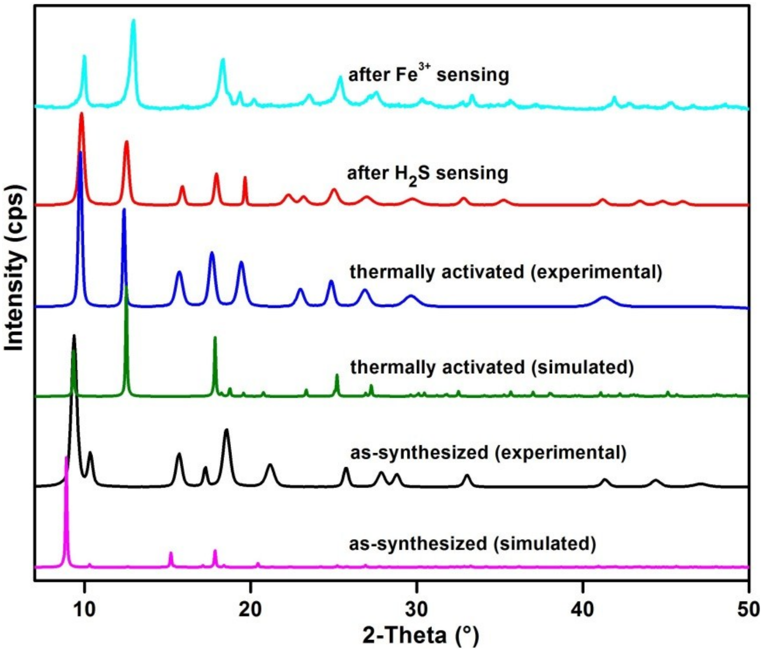

**Figure S1.** XRPD patterns of **1** in different forms: as-synthesized, thermally activated, after sensing of $H_2S$ and Fe$^{3+}$ ion.

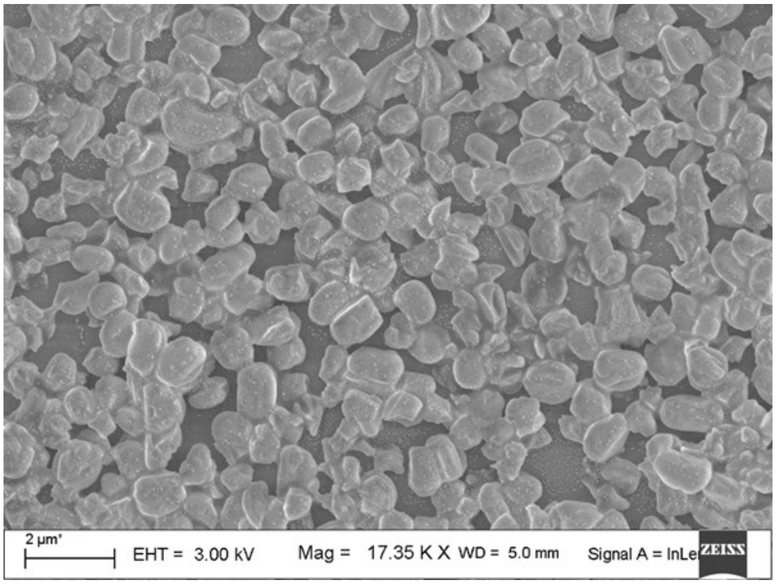

**Figure S2.** FE-SEM images of **1′**.

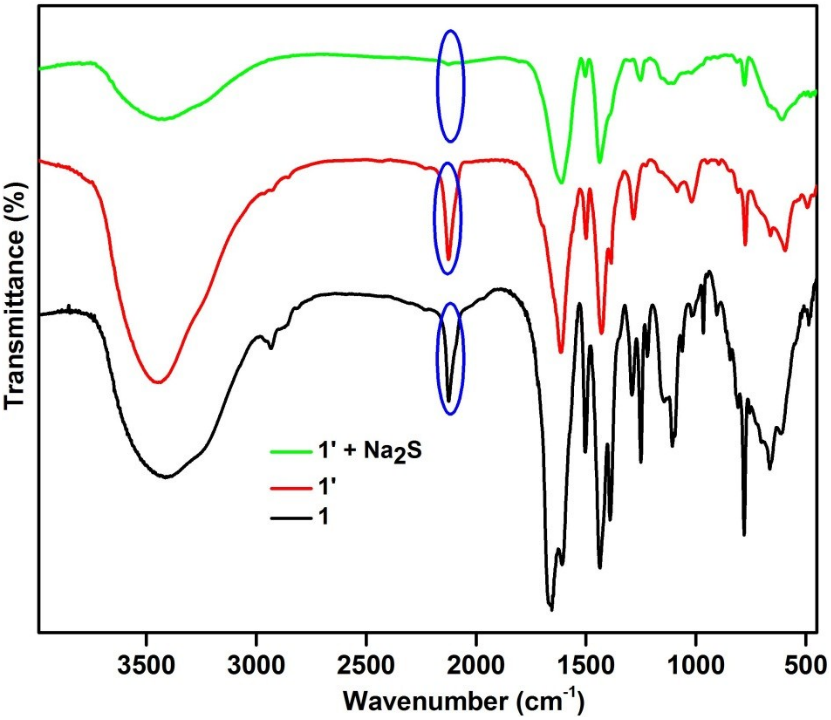

**Figure S3.** FT-IR spectra of as-synthesized **1** (black), thermally activated (red) **1'**, and **1'** after treatment with $Na_2S$ (green). The absorption band for the $–N_3$ group is high-lighted by the blue ovals.

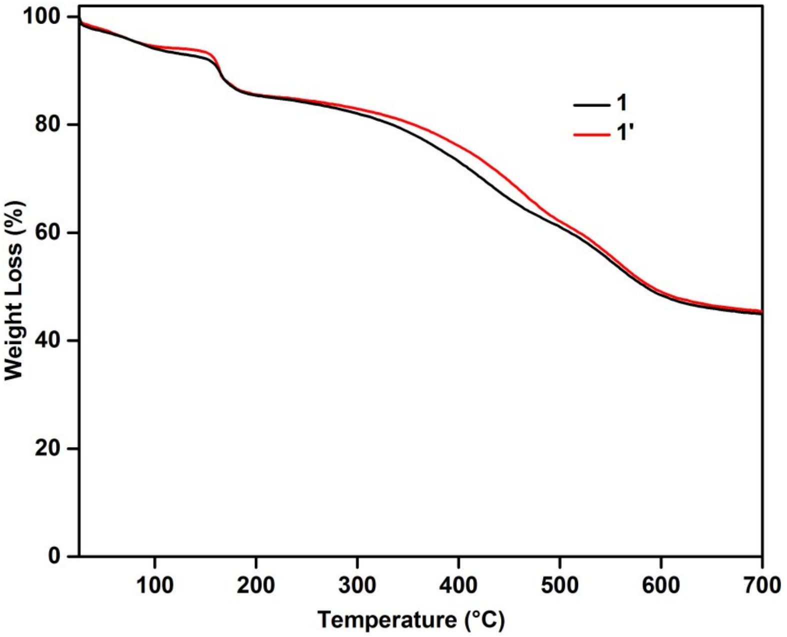

**Figure S4.** TG curves of as-synthesized **1** (black) and thermally activated **1′** (red) recorded in an air atmosphere in the temperature range of 25-700 °C with a heating rate of 10 °C $min^{-1}$.

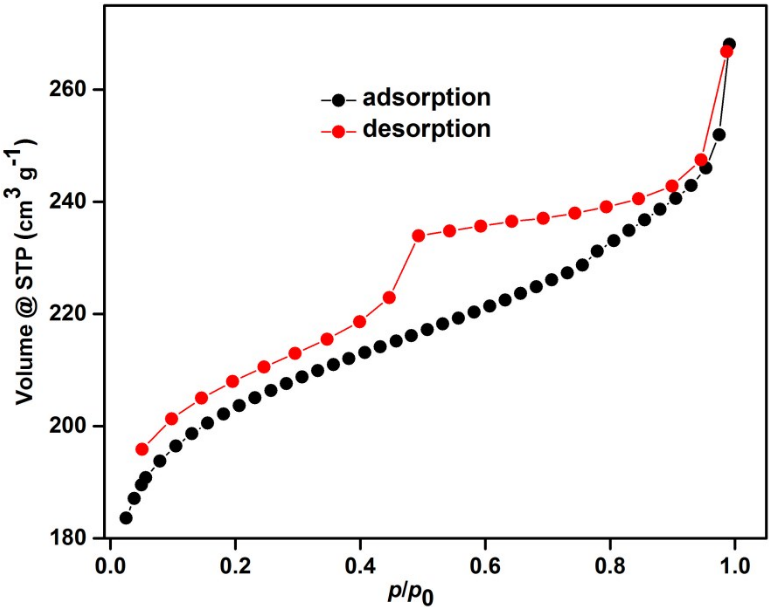

**Figure S5.** $N_2$ adsorption (black circles) and desorption (red circles) isotherms of **1′** measured at –196 °C.

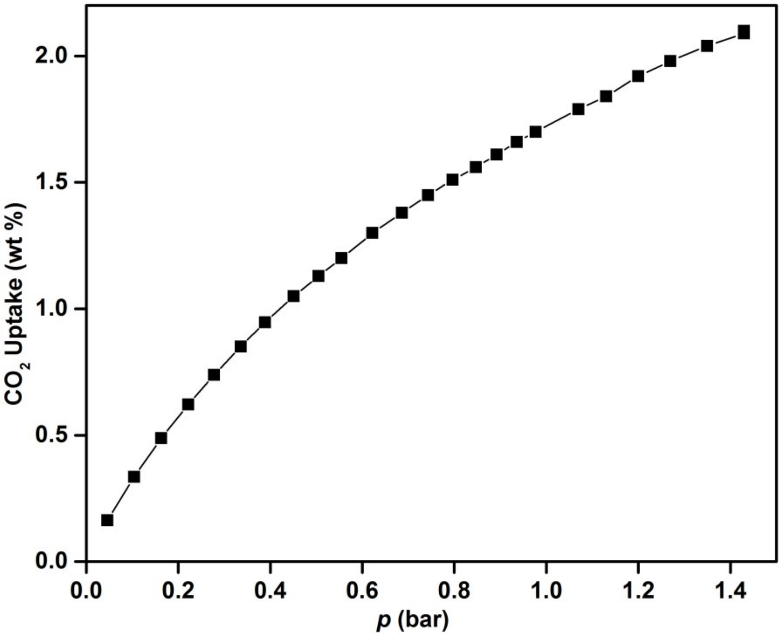

**Figure S6.** $CO_2$ adsorption isotherms of **1′** measured at 25 °C.

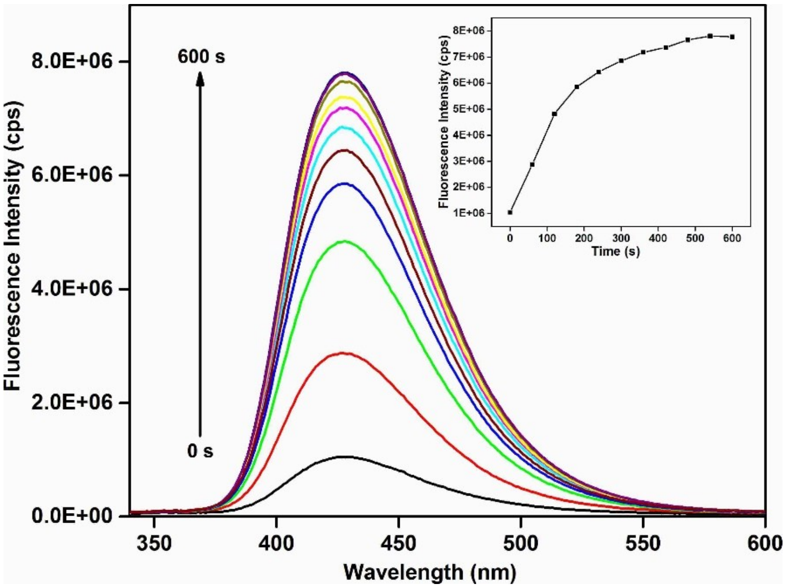

**Figure S7.** Fluorescence turn-on response of **1′** (in HEPES buffer) towards the addition of $Na_2S$ at a regular time interval (60 s) up to 600 s. Inset: time-dependence of fluorescence intensity at 425 nm.

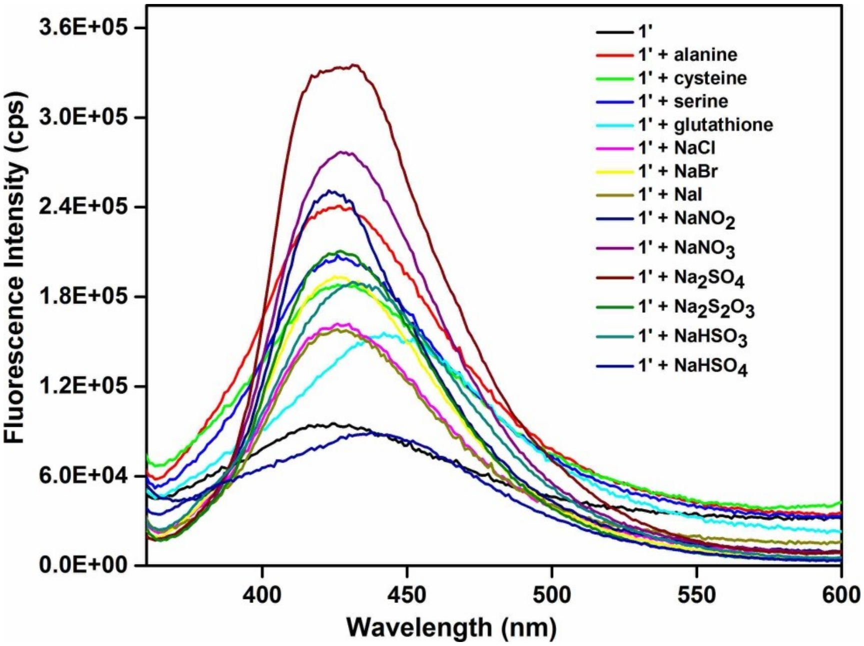

**Figure S8.** Fluorescence response of **1′** in presence of different analytes in water.

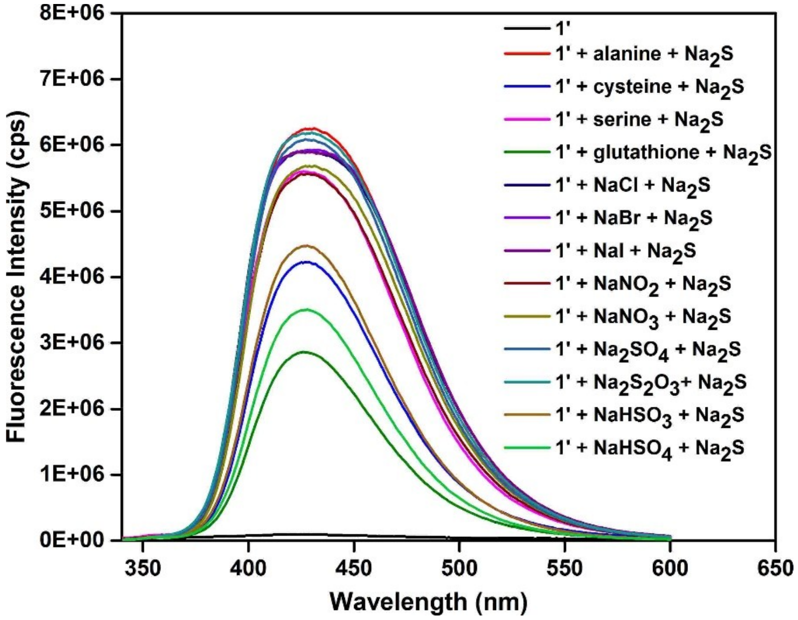

**Figure S9.** Fluorescence response of **1′** towards $Na_2S$ in presence of other interfering analytes in water.

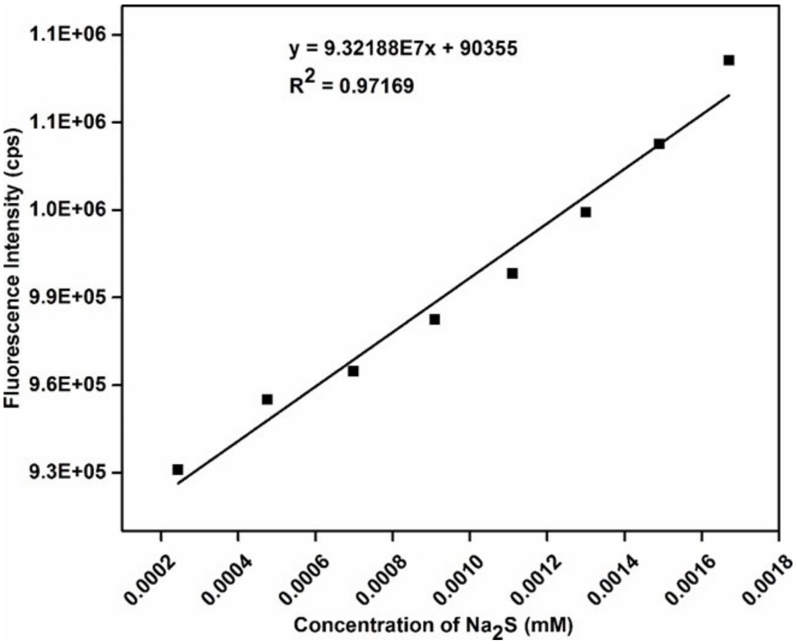

**Figure S10.** Change in the fluorescence intensity of **1′** in aqueous suspension as a function of $Na_2S$ concentration.

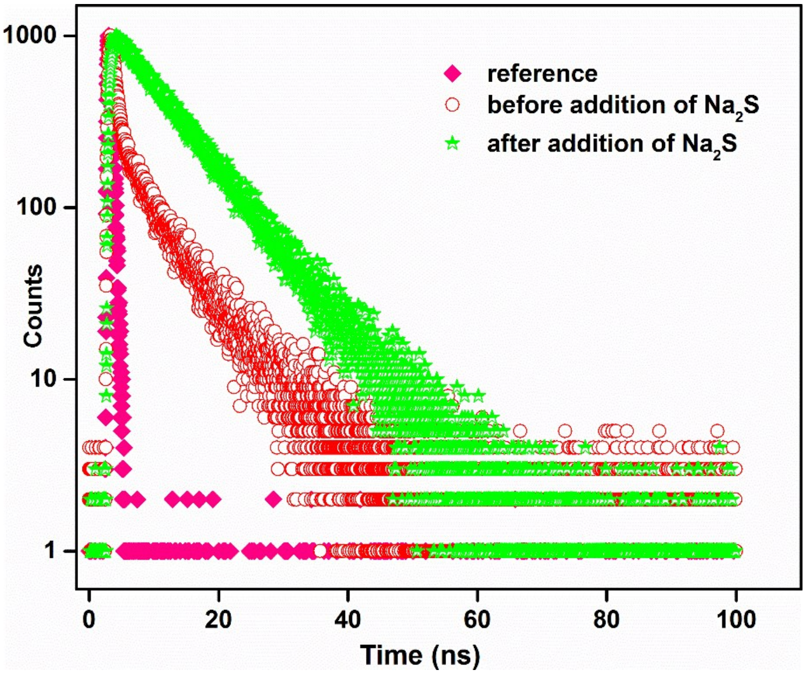

**Figure 11.** Lifetime decay profile of **1′** before and after addition of 100 μL of 0.21 (M) $Na_2S$ solution.

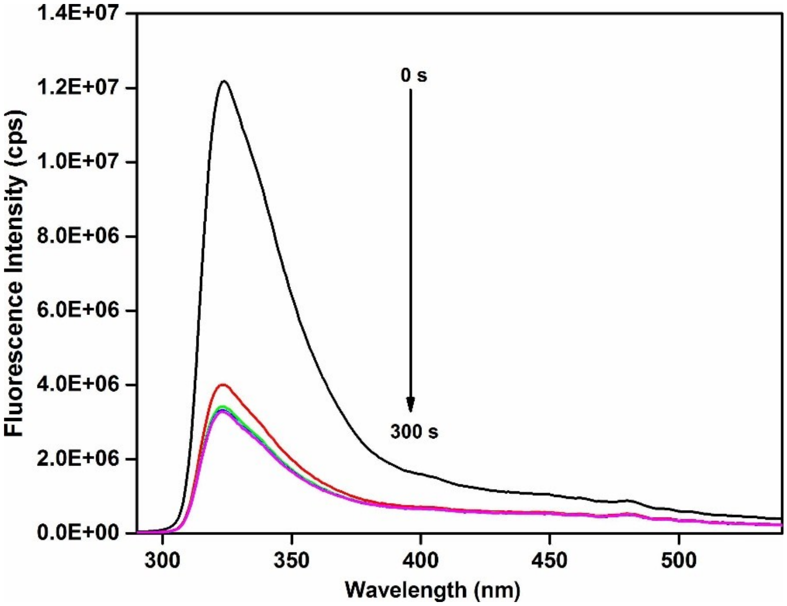

**Figure S12.** Fluorescence turn-off response of Al-MIL-53 (in aqueous medium) towards the addition of $Na_2S$ at a regular time interval (60 s) up to 300 s.

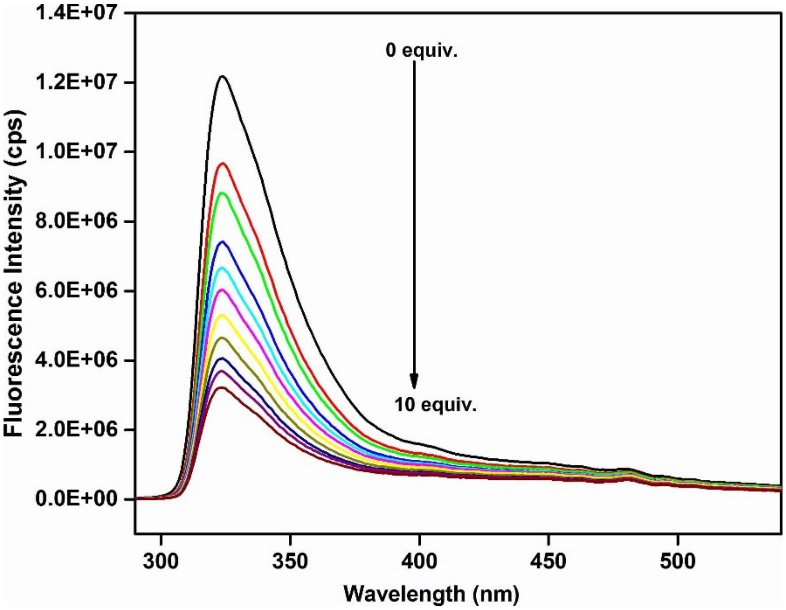

**Figure S13.** Change in fluorescence intensity of Al-MIL-53 (in aqueous medium) with increasing concentration of $Na_2S$ (up to 10 equiv.).

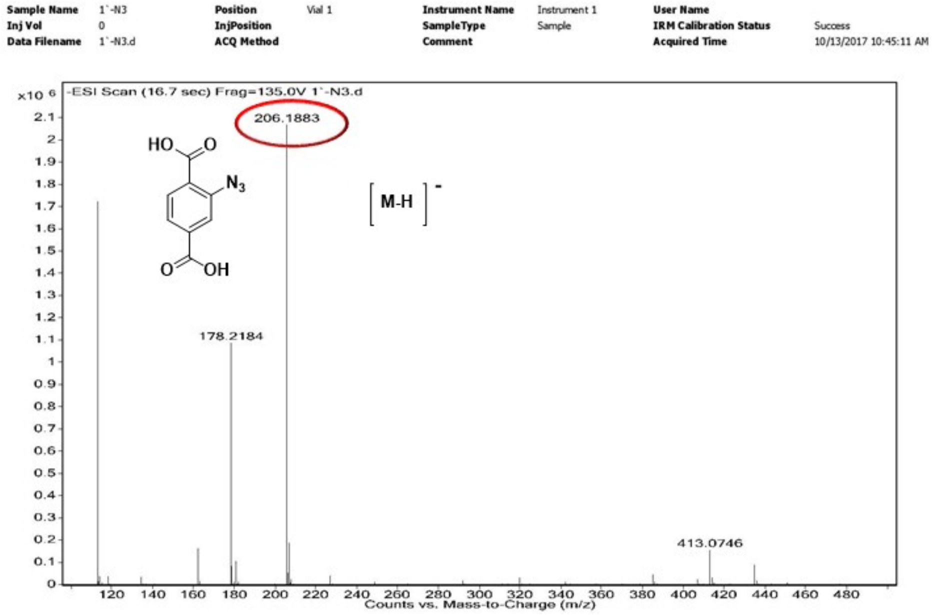

| | | | | | | | |
|---|---|---|---|---|---|---|---|
| **Sample Name** | 1`-N3 | **Position** | Vial 1 | **Instrument Name** | Instrument 1 | **User Name** | |
| **Inj Vol** | 0 | **InjPosition** | | **SampleType** | Sample | **IRM Calibration Status** | Success |
| **Data Filename** | 1`-N3.d | **ACQ Method** | | **Comment** | | **Acquired Time** | 10/13/2017 10:45:11 AM |

**Figure S14.** HR-MS spectrum of **1′** after digestion in MeOH/HF. The spectrum shows m/z (negative ion mode) peak at 206.1883 (negative ion mode), which corresponds to $(M\text{-}H)^-$ ion (M = mass of $H_2BDC\text{-}N_3$ ligand).

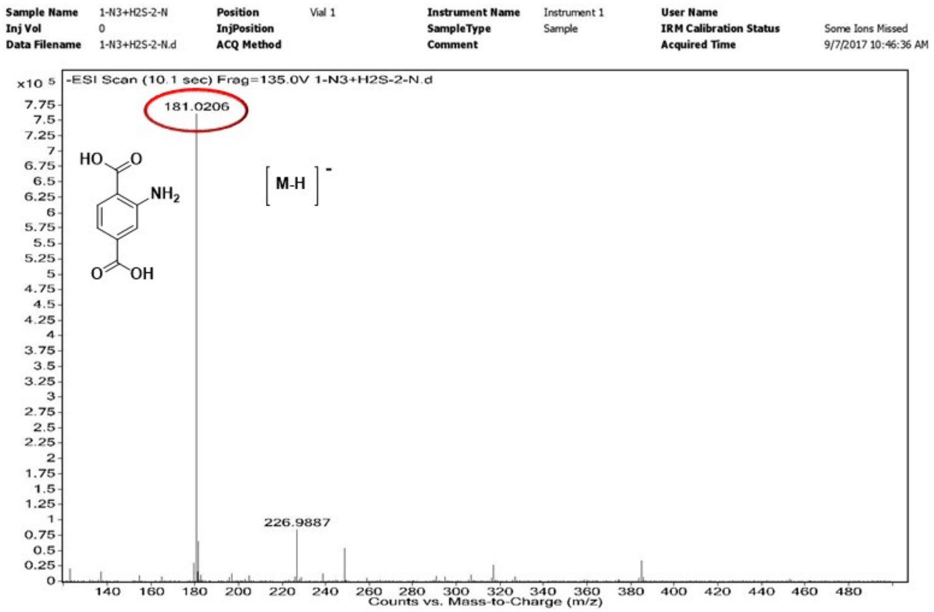

| | | | | | | | |
|---|---|---|---|---|---|---|---|
| **Sample Name** | 1-N3+H2S-2-N | **Position** | Vial 1 | **Instrument Name** | Instrument 1 | **User Name** | |
| **Inj Vol** | 0 | **InjPosition** | | **SampleType** | Sample | **IRM Calibration Status** | Some Ions Missed |
| **Data Filename** | 1-N3+H2S-2-N.d | **ACQ Method** | | **Comment** | | **Acquired Time** | 9/7/2017 10:46:36 AM |

**Figure S15.** HR-MS spectrum of $Na_2S$-treated **1′** after digestion in MeOH/HF. The spectrum shows m/z (negative ion mode) peak at 181.0206 which correspond to $(M-H)^-$ ion of reduced $H_2BDC-N_3$ i.e. $H_2BDC-NH_2$ ligand.

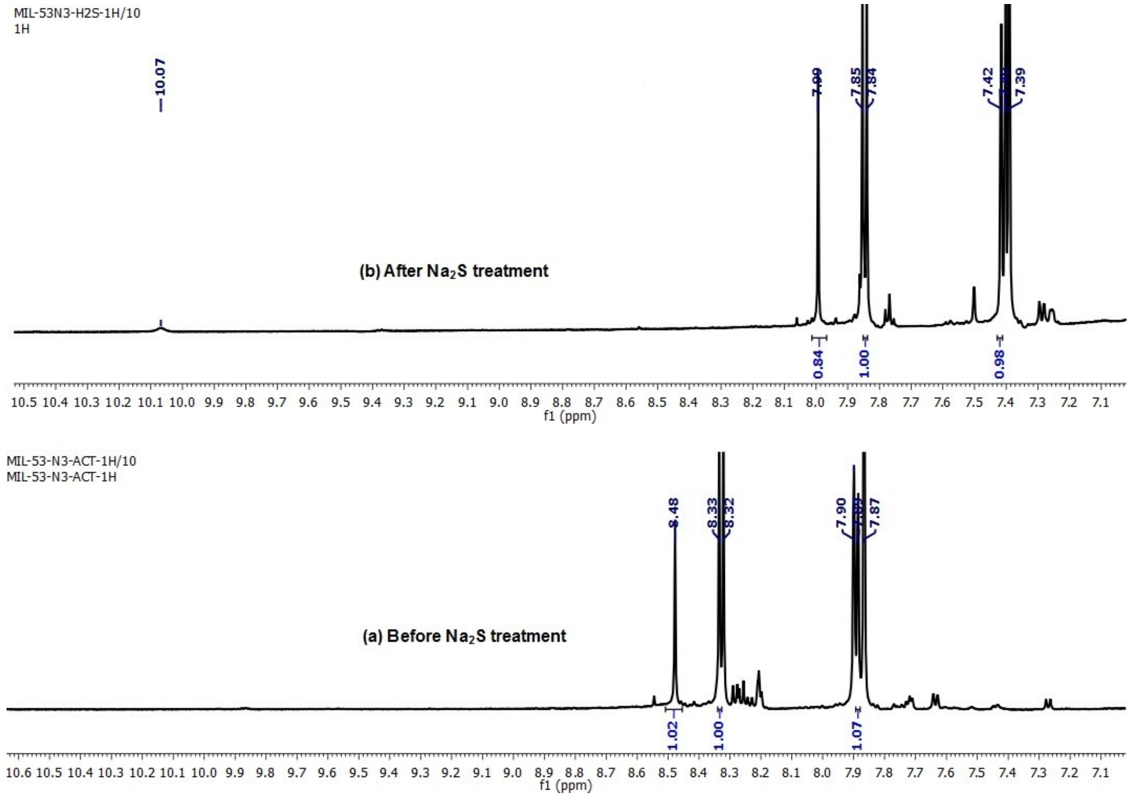

**Figure S16.** $^1H$ NMR spectra of (a) **1′** and (b) $Na_2S$-treated **1′** after digestion in DMSO-$d_6$/HF. In the spectrum of $Na_2S$-treated **1′**, a new peak appears at 10.07 ppm, which can be assigned to the protons for the–$NH_3^+$ group attached with the protonated form of $H_2BDC-NH_2$ ligand.

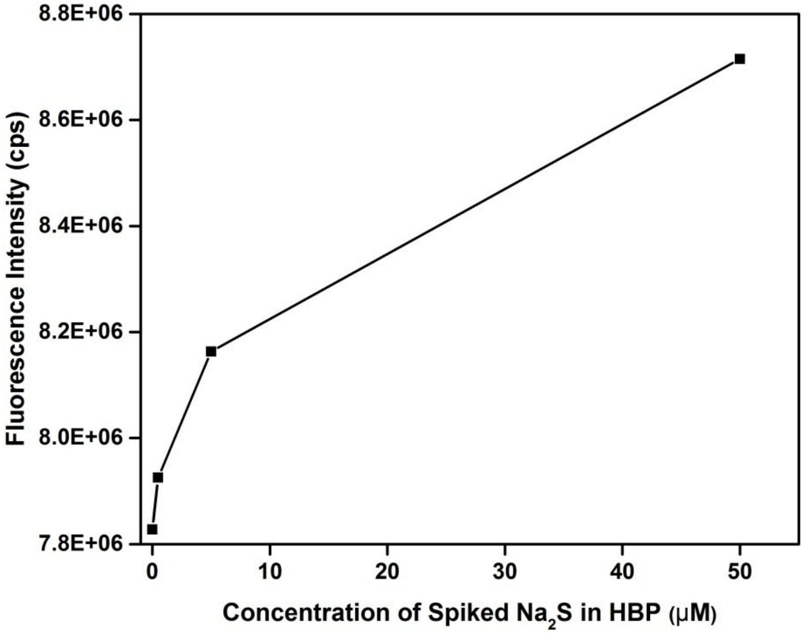

**Figure S17.** Fluorescence response of **1′** in presence of $Na_2S$-spiked human blood plasma.

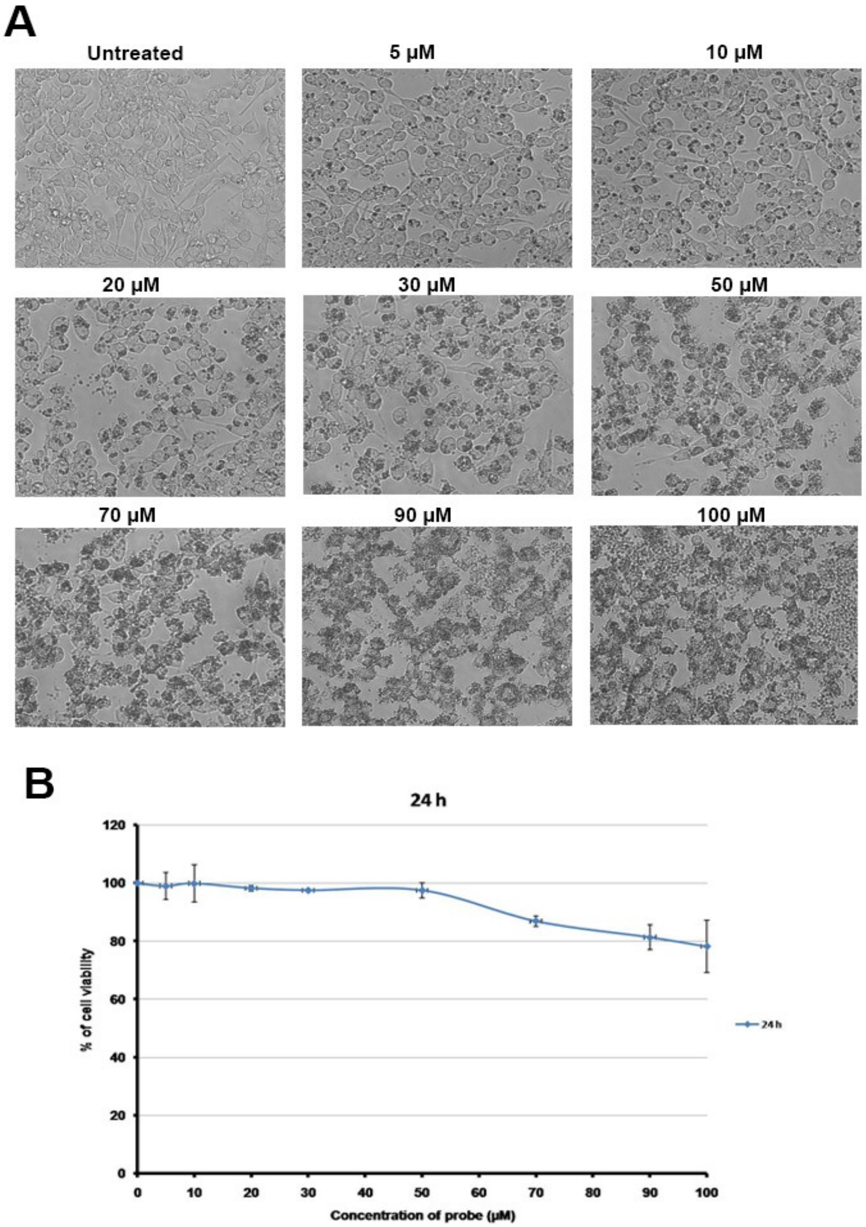

**Figure S18.** Cell viability in **1′** - treated J774A.1 cells: (A) The cells either remained untreated or treated with the probe (0-100 μM) for a period of 24 h and the change in morphology was monitored. The shape of the **1′** - treated cells was found intact even at 100 μM concentration of the probe. (B) The MTT assay was performed and the cells treated with the probe showed almost 100% cell viability (the data is representative of three independent experiments).

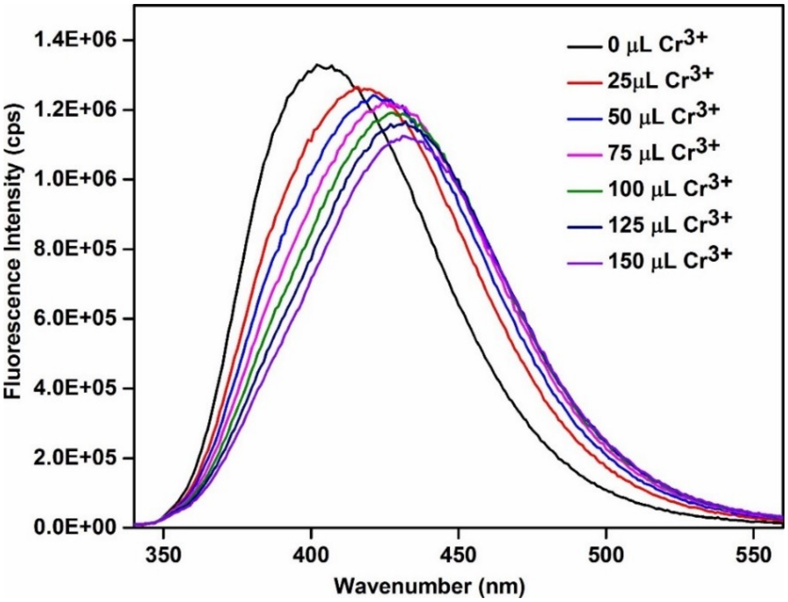

**Figure S19.** Change in the fluorescence intensity of **1′** upon incremental addition of 2 mM $Cr^{3+}$ solution.

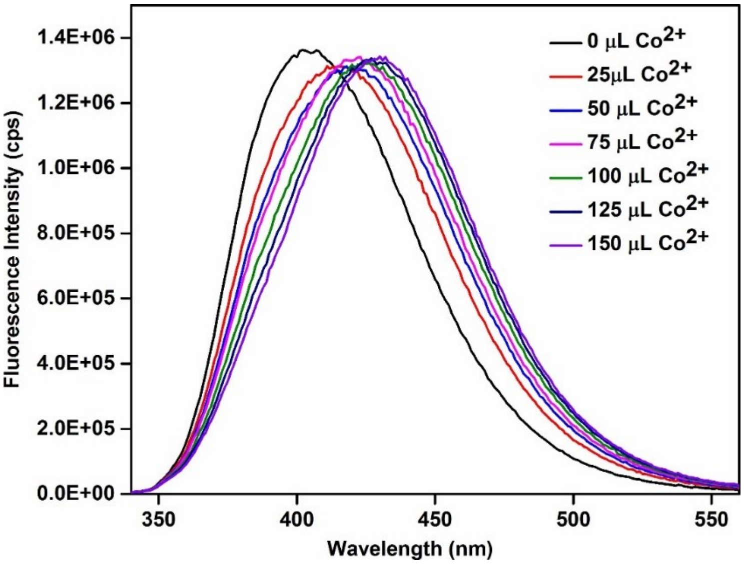

**Figure S20.** Change in the fluorescence intensity of **1′** upon incremental addition of 2 mM $Co^{2+}$ solution.

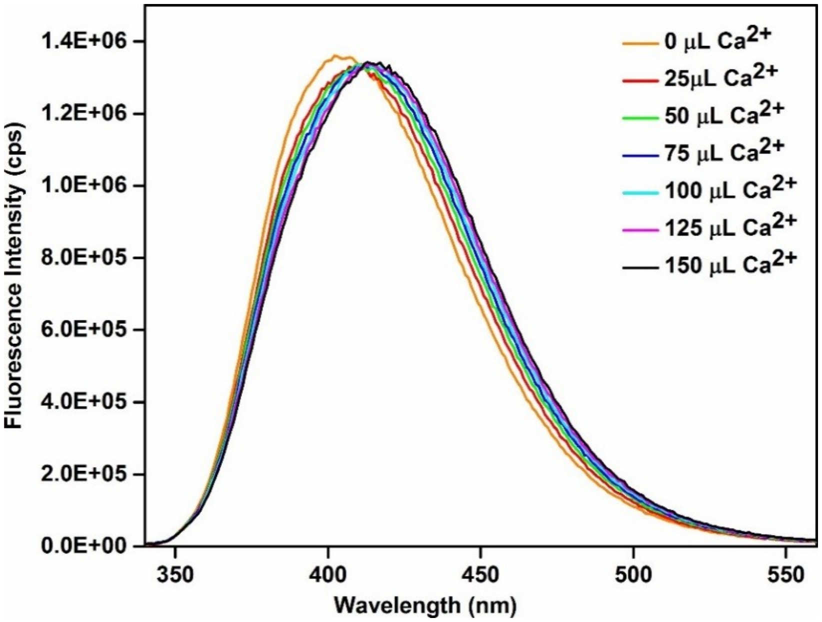

**Figure S21.** Change in the fluorescence intensity of **1′** upon incremental addition of 2 mM $Ca^{2+}$ solution.

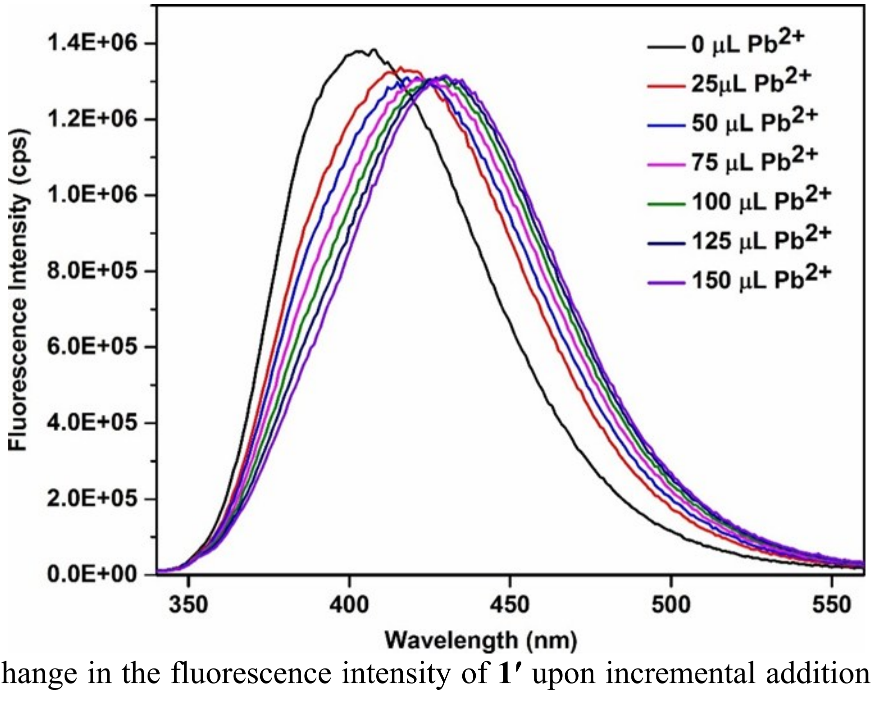

**Figure S22.** Change in the fluorescence intensity of **1′** upon incremental addition of 2 mM $Pb^{2+}$ solution.

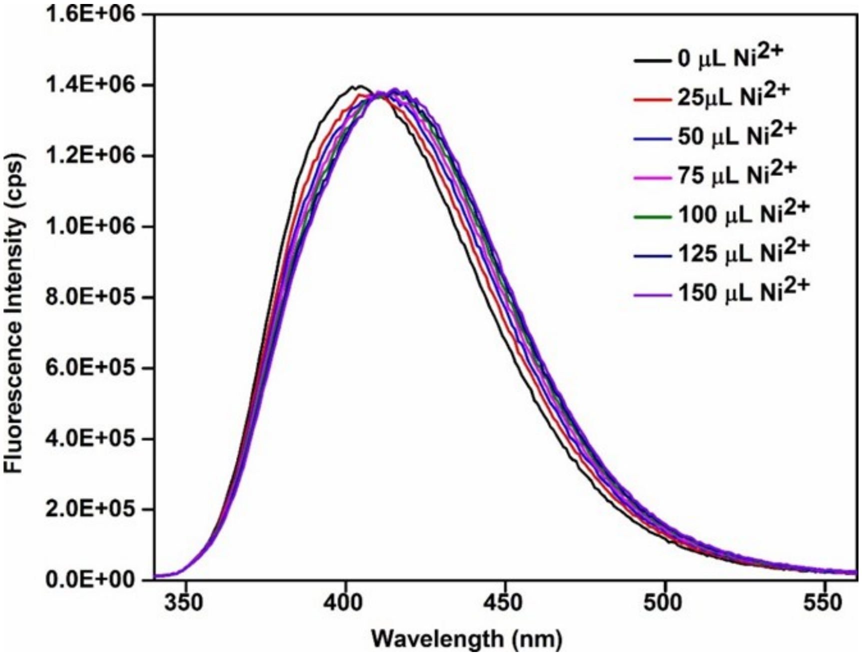

**Figure S23.** Change in the fluorescence intensity of **1′** upon incremental addition of 2 mM $Ni^{2+}$ solution.

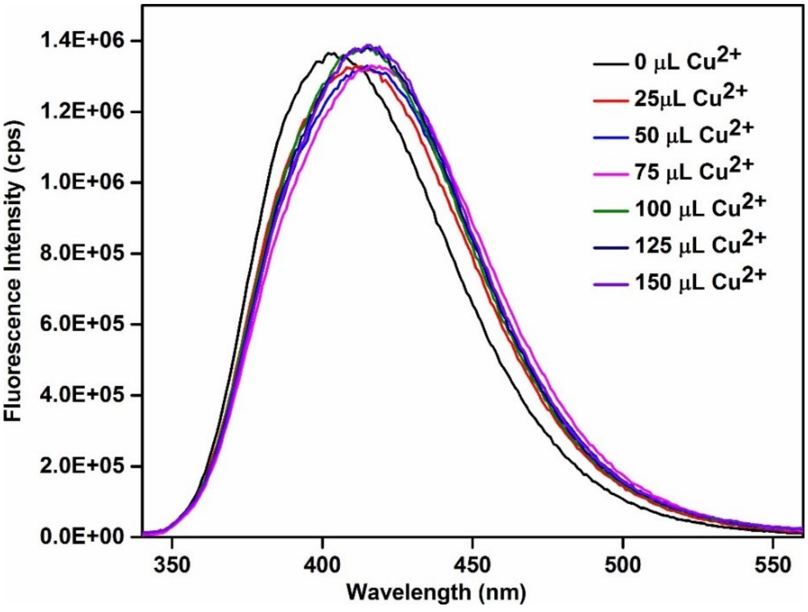

**Figure S24.** Change in the fluorescence intensity of **1′** upon incremental addition of 2 mM $Cu^{2+}$ solution.

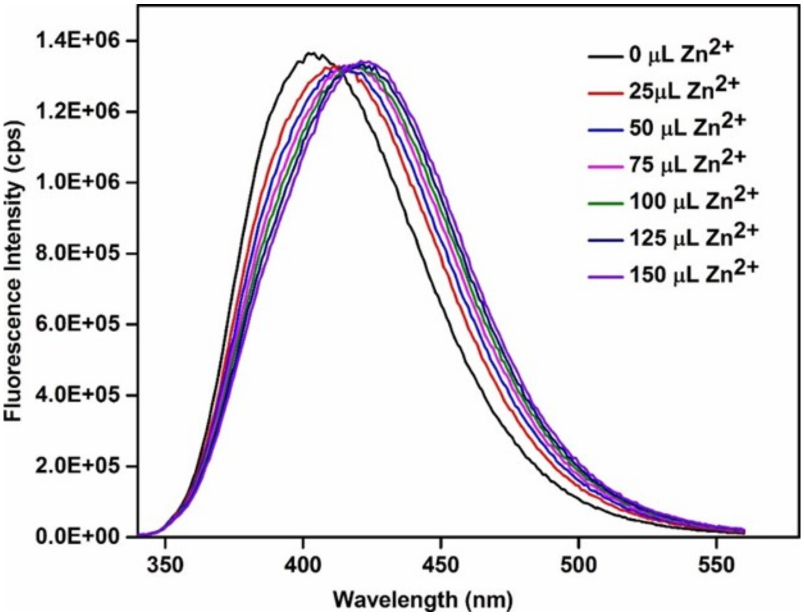

**Figure S25.** Change in the fluorescence intensity of **1′** upon incremental addition of 2 mM $Zn^{2+}$ solution

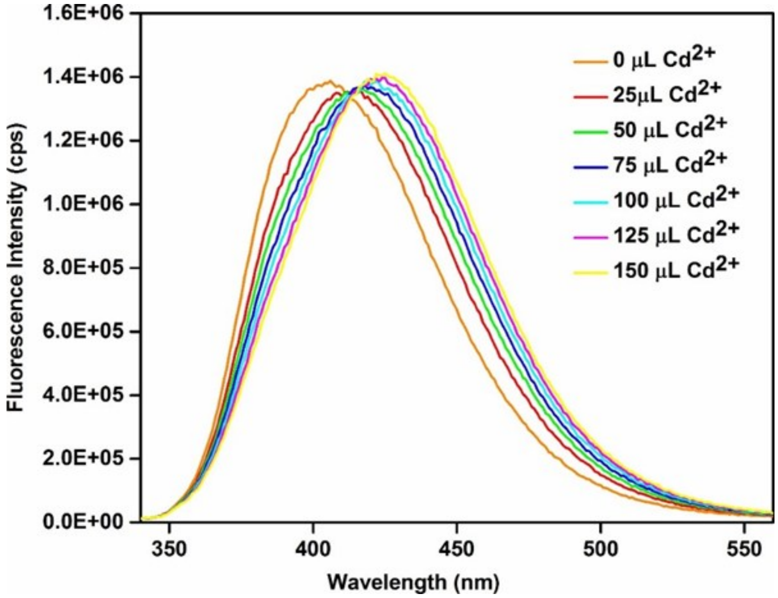

**Figure S26.** Change in the fluorescence intensity of **1′** upon incremental addition of 2 mM $Cd^{2+}$ solution.

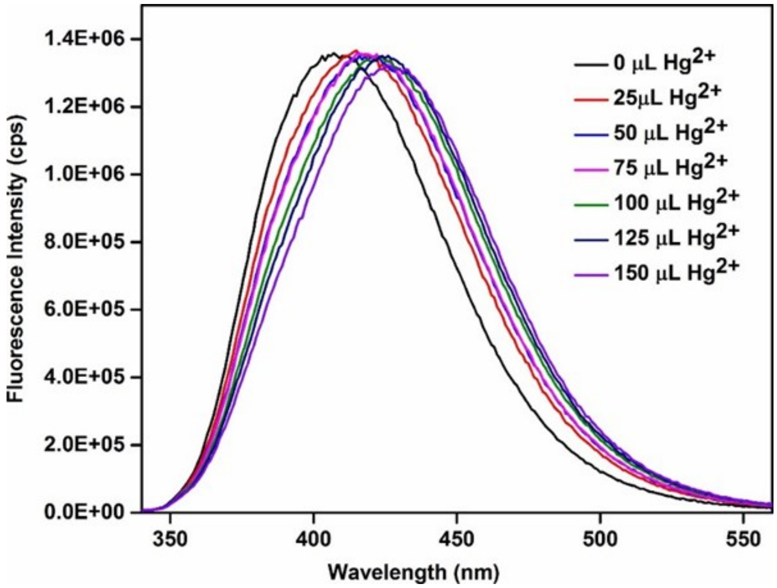

**Figure S27.** Change in the fluorescence intensity of **1′** upon incremental addition of 2 mM $Hg^{2+}$ solution.

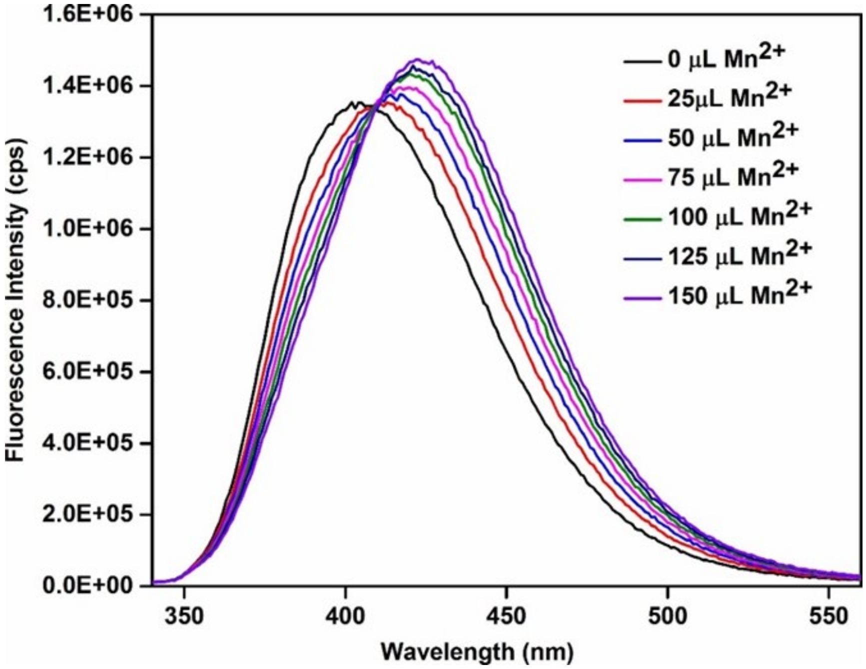

**Figure S28.** Change in the fluorescence intensity of **1′** upon incremental addition of 2 mM $Mn^{2+}$ solution.

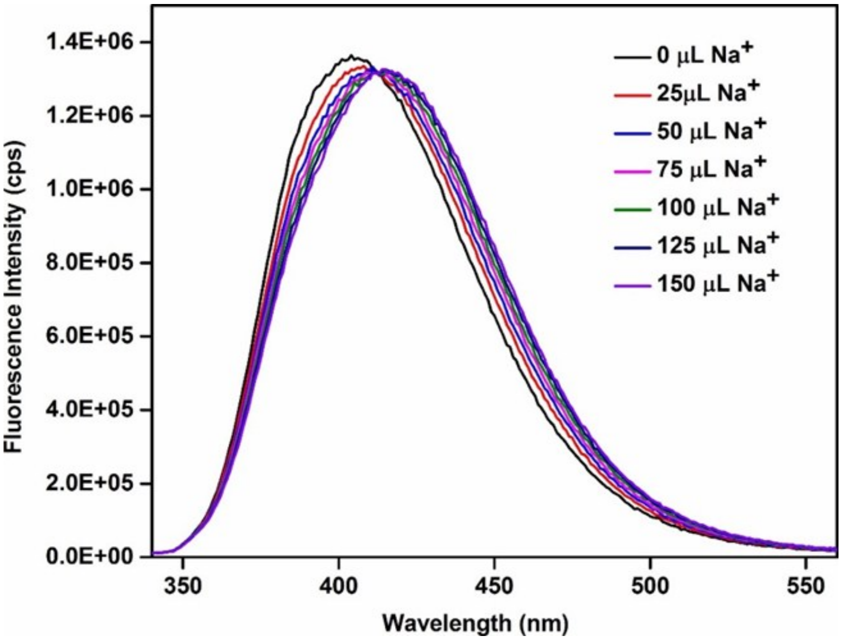

**Figure S29.** Change in the fluorescence intensity of **1′** upon incremental addition of 2 mM $Na^+$ solution.

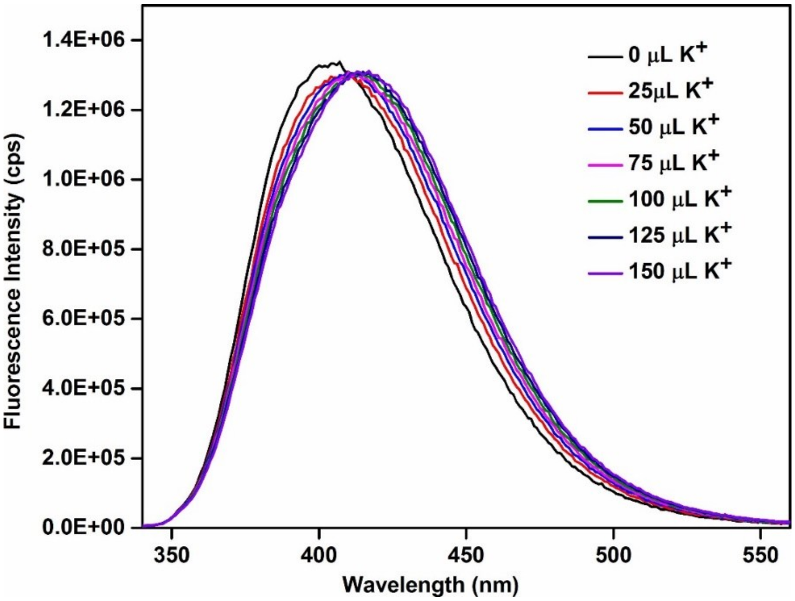

**Figure S30.** Change in the fluorescence intensity of **1′** upon incremental addition of 2 mM $K^+$ solution.

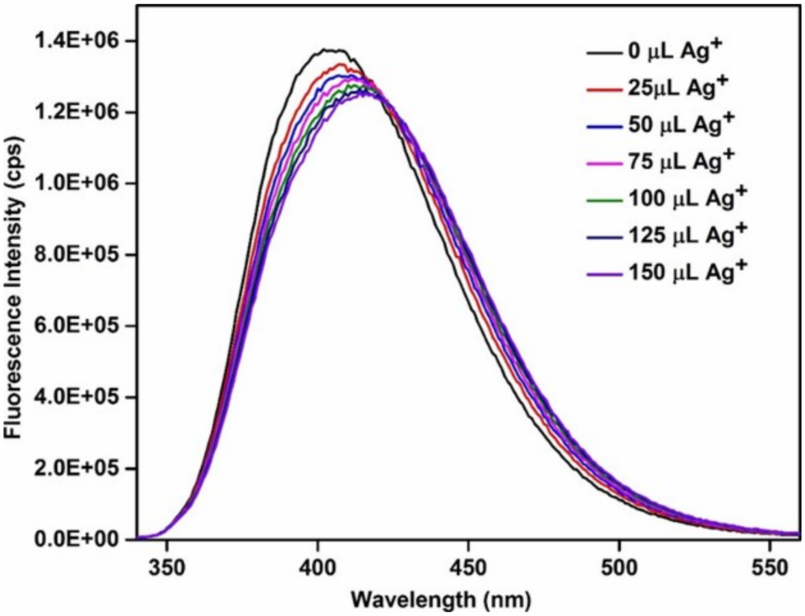

**Figure S31.** Change in the fluorescence intensity of **1′** upon incremental addition of 2 mM $Ag^+$ solution.

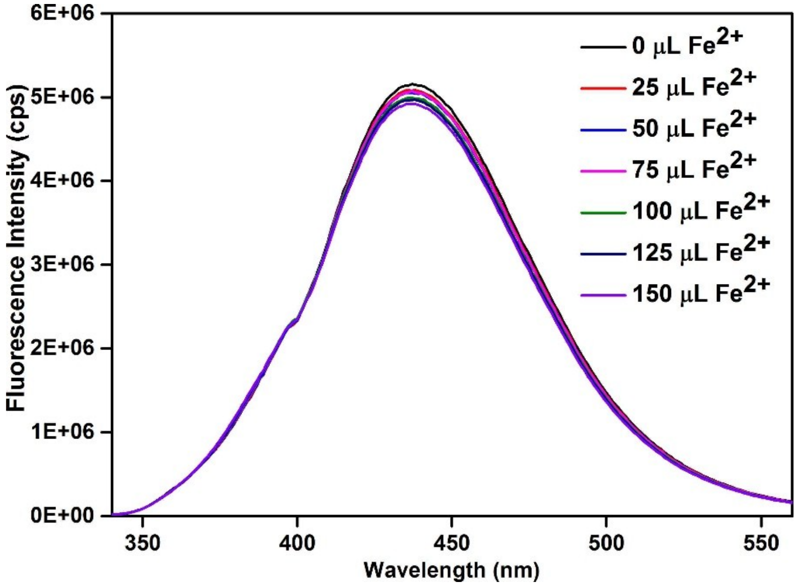

**Figure S32.** Change in the fluorescence intensity of **1′** upon incremental addition of 2 mM $Fe^{2+}$ solution.

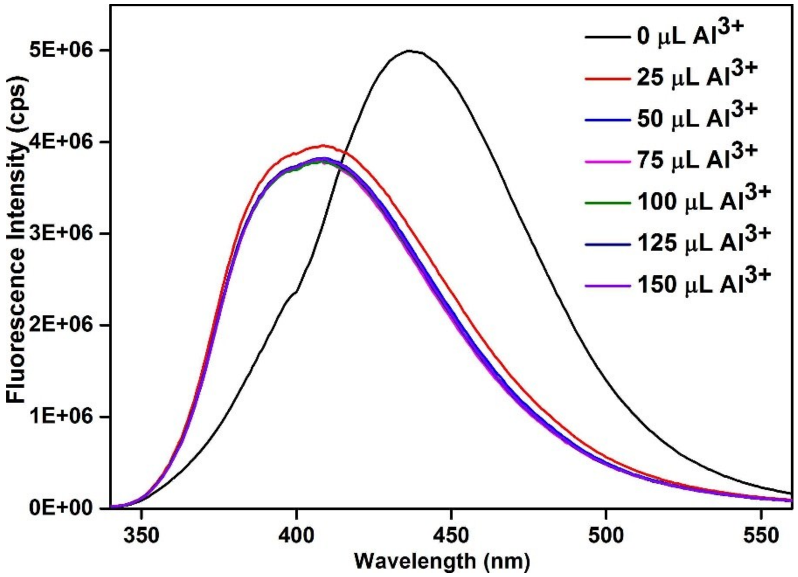

**Figure S33.** Change in the fluorescence intensity of **1′** upon incremental addition of 2 mM $Al^{3+}$ solution.

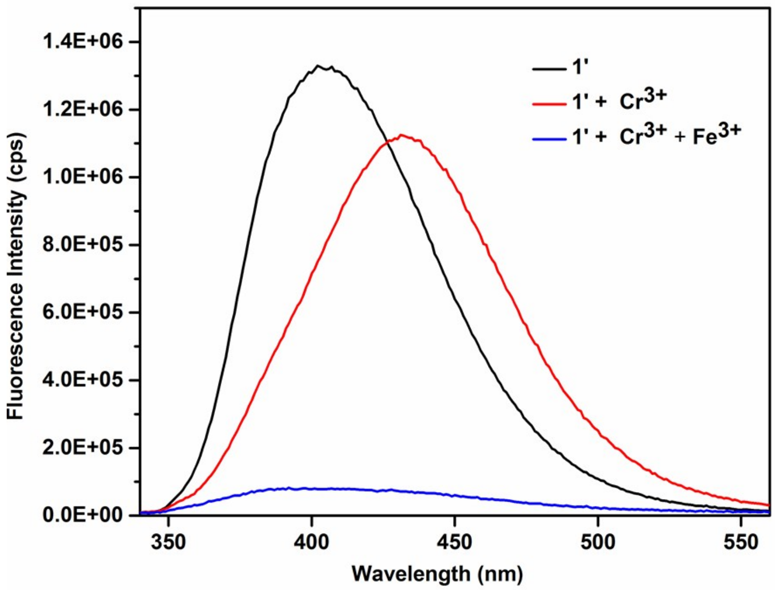

**Figure S34.** Change in the fluorescence intensity of **1′** upon addition of 2 mM $Cr^{3+}$ solution (150 μL) in presence of $Fe^{3+}$ (150 μL) solution.

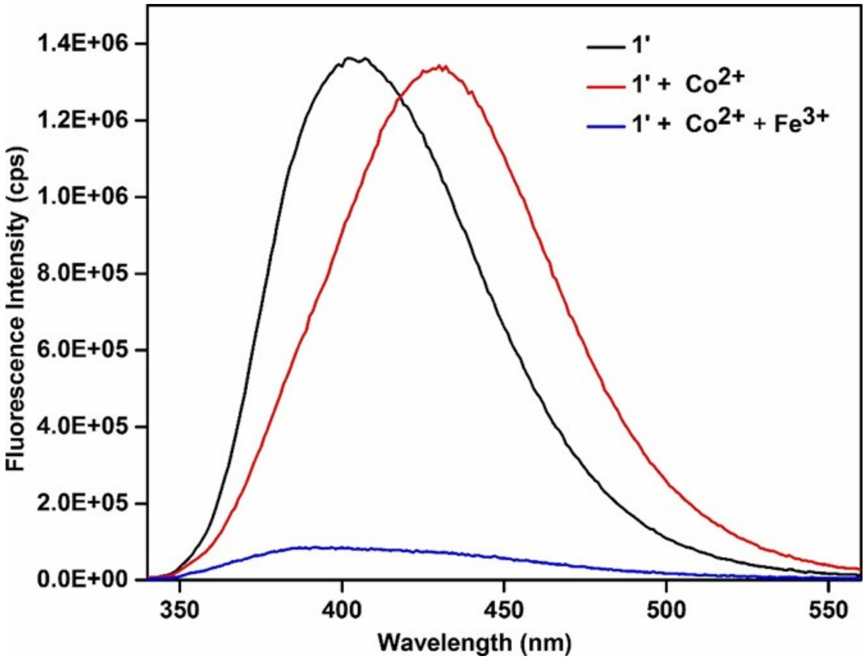

**Figure S35.** Change in the fluorescence intensity of **1′** upon addition of 2 mM $Co^{2+}$ solution (150 μL) in presence of $Fe^{3+}$ (150 μL) solution.

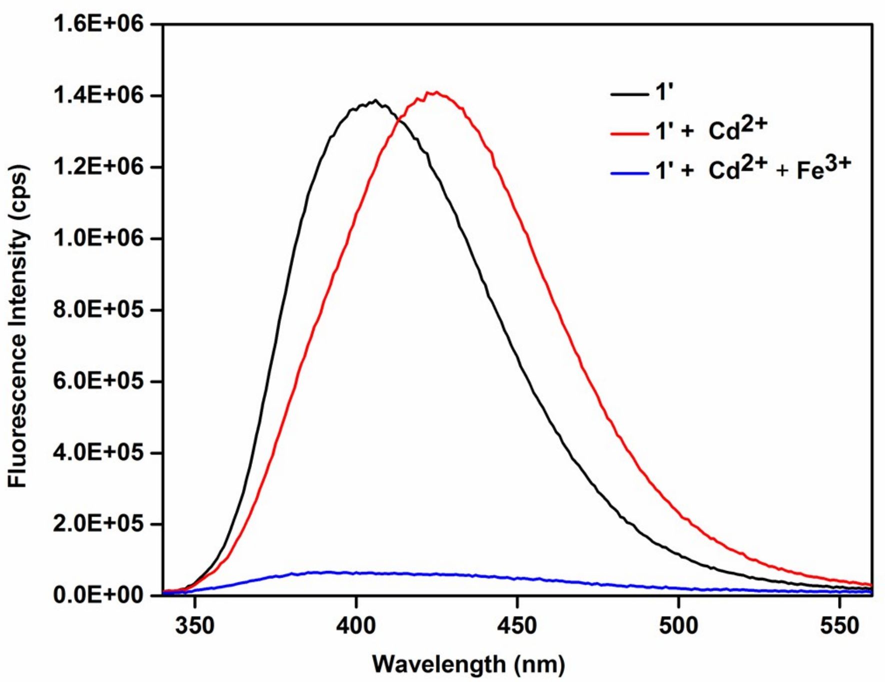

**Figure S36.** Change in the fluorescence intensity of **1′** upon addition of 2 mM $Cd^{2+}$ solution (150 μL) in presence of $Fe^{3+}$ (150 μL) solution.

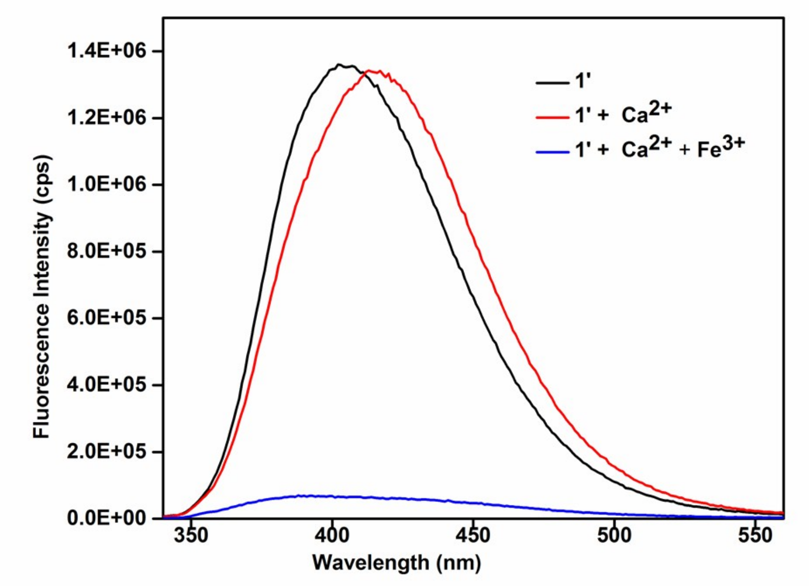

**Figure S37.** Change in the fluorescence intensity of **1′** upon addition of 2 mM $Ca^{2+}$ solution (150 μL) in presence of $Fe^{3+}$ (150 μL) solution.

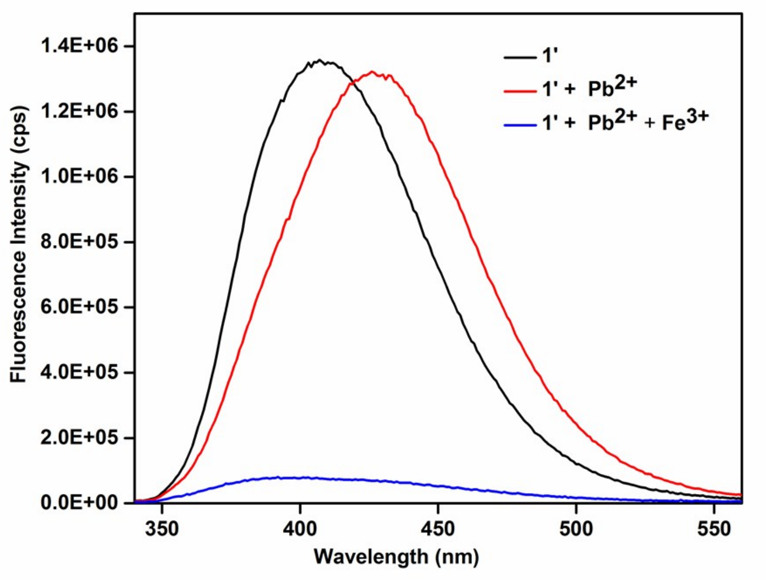

**Figure S38.** Change in the fluorescence intensity of **1′** upon addition of 2 mM $Pb^{2+}$ solution (150 μL) in presence of $Fe^{3+}$ (150 μL) solution.

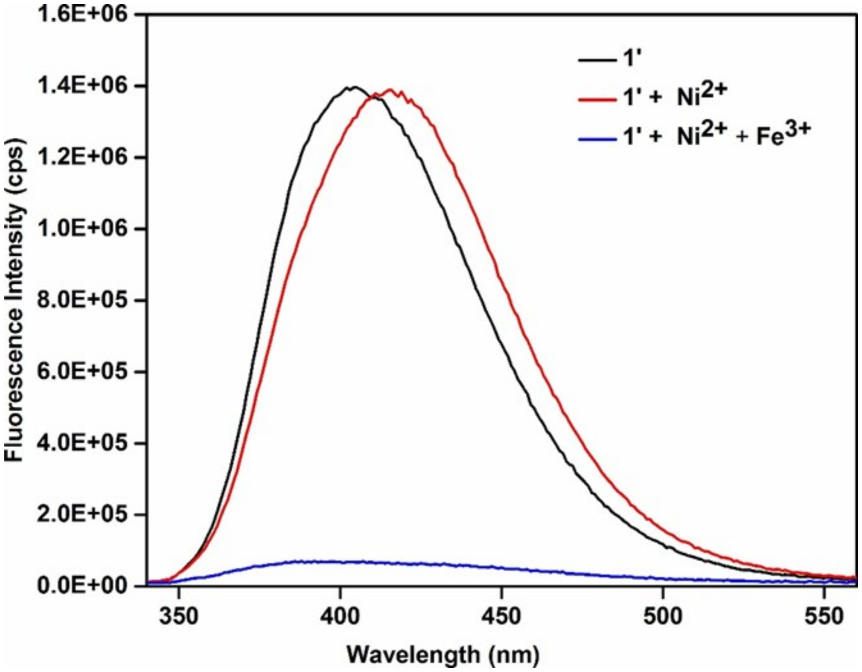

**Figure S39.** Change in the fluorescence intensity of **1′** upon addition of 2 mM $Ni^{2+}$ solution (150 μL) in presence of $Fe^{3+}$ (150 μL) solution.

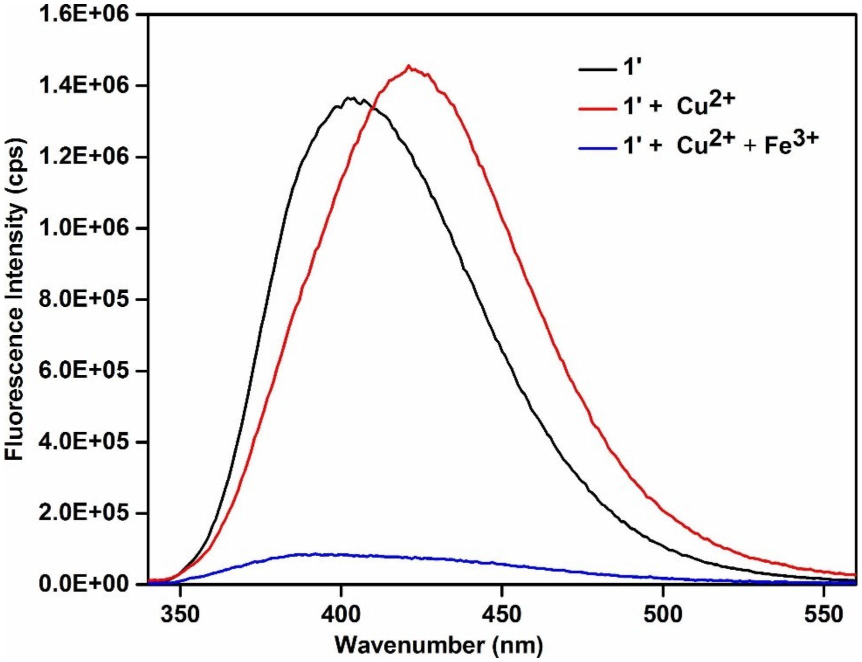

**Figure S40.** Change in the fluorescence intensity of **1′** upon addition of 2 mM $Cu^{2+}$ solution (150 μL) in presence of $Fe^{3+}$ (150 μL) solution.

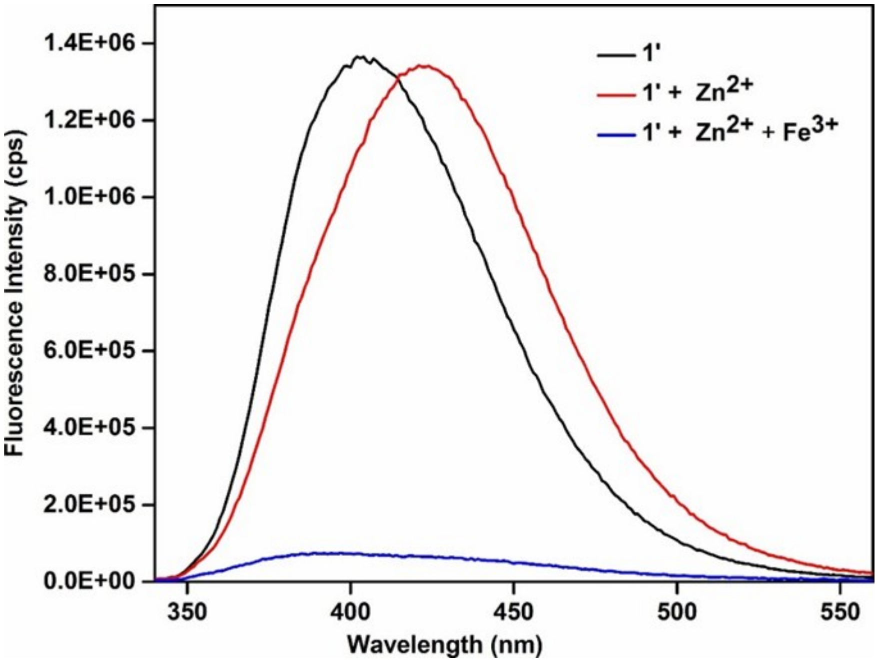

**Figure S41.** Change in the fluorescence intensity of **1′** upon addition of 2 mM $Zn^{2+}$ solution (150 μL) in presence of $Fe^{3+}$ (150 μL) solution.

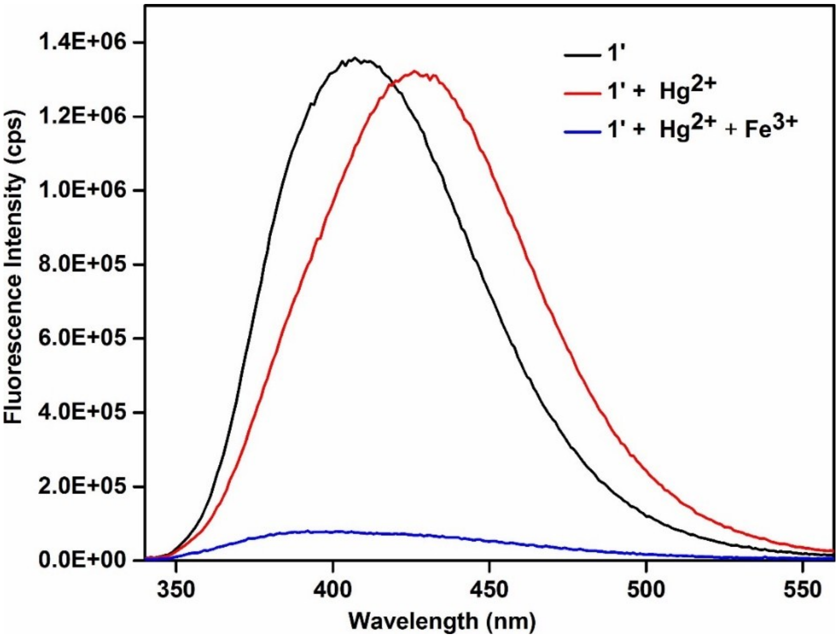

**Figure S42.** Change in the fluorescence intensity of **1′** upon addition of 2 mM $Hg^{2+}$ solution (150 μL) in presence of $Fe^{3+}$ (150 μL) solution.

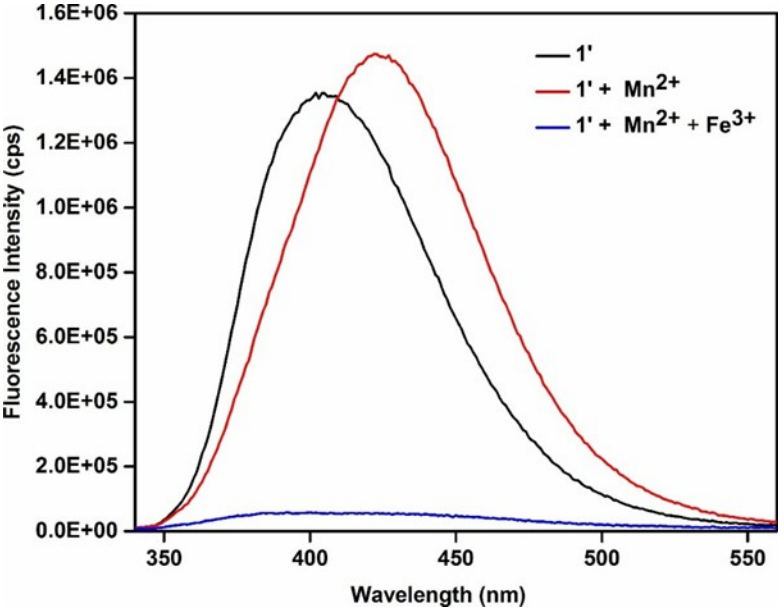

**Figure S43.** Change in the fluorescence intensity of **1′** upon addition of 2 mM $Mn^{2+}$ solution (150 μL) in presence of $Fe^{3+}$ (150 μL) solution.

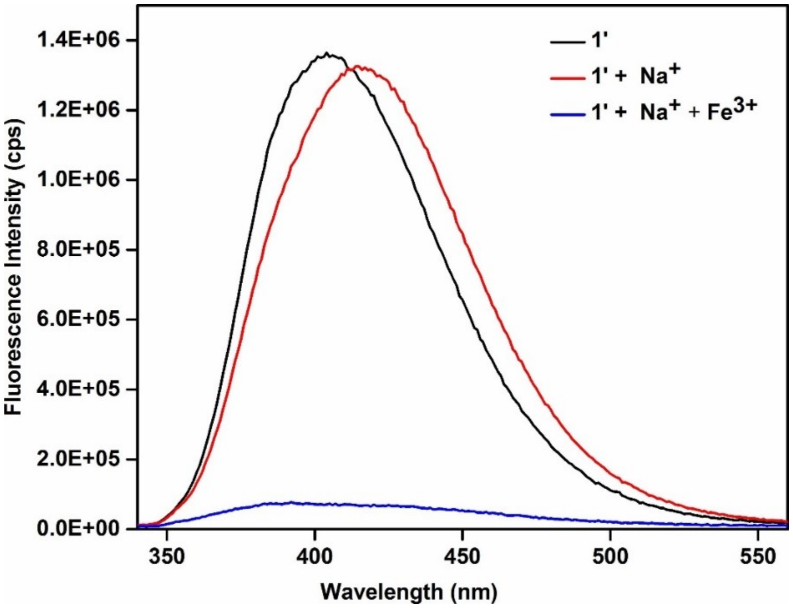

**Figure S44.** Change in the fluorescence intensity of **1′** upon addition of 2 mM $Na^{+}$ solution (150 μL) in presence of $Fe^{3+}$ (150 μL) solution.

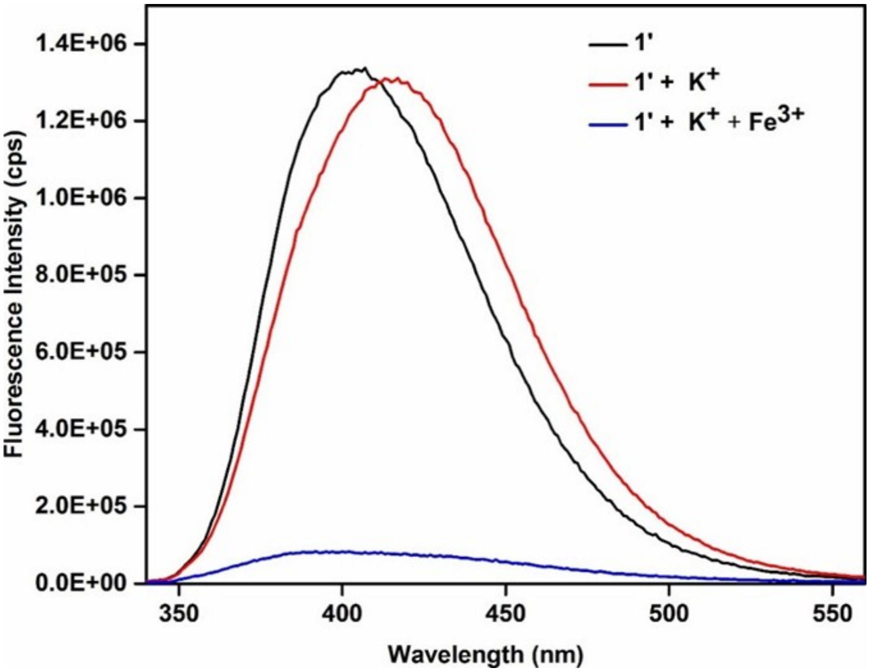

**Figure S45.** Change in the fluorescence intensity of **1′** upon addition of 2 mM $K^+$ solution (150 μL) in presence of $Fe^{3+}$ (150 μL) solution.

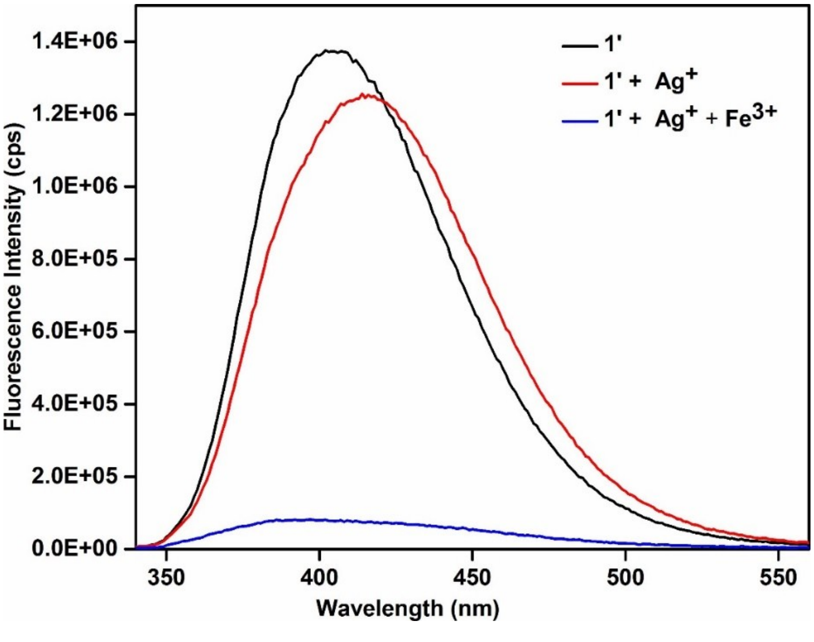

**Figure S46.** Change in the fluorescence intensity of **1′** upon addition of 2 mM $Ag^+$ solution (150 μL) in presence of $Fe^{3+}$ (150 μL) solution.

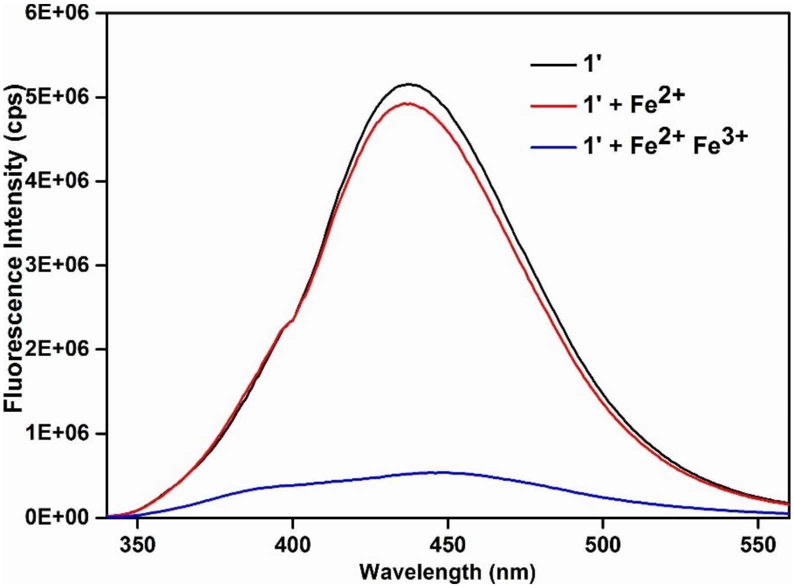

**Figure S47.** Change in the fluorescence intensity of **1′** upon addition of 2 mM $Fe^{2+}$ solution (150 μL) in presence of $Fe^{3+}$ (150 μL) solution.

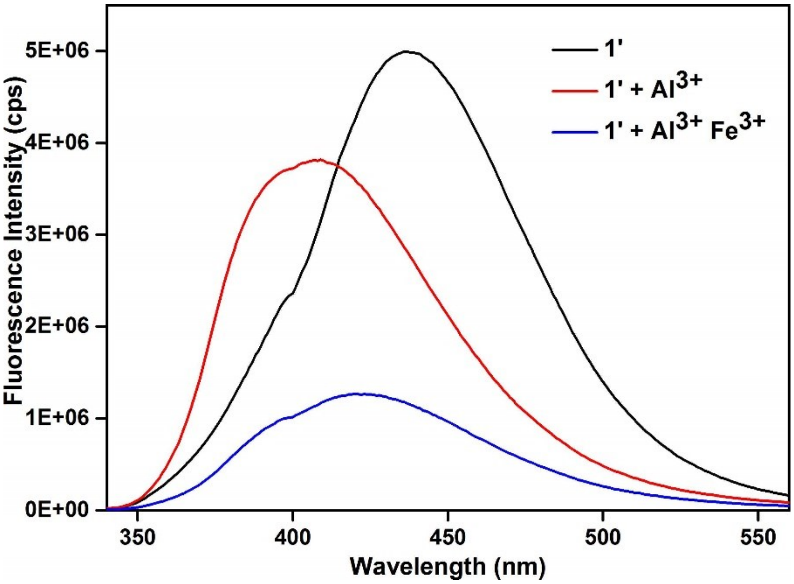

**Figure S48.** Change in the fluorescence intensity of **1′** upon addition of 2 mM $Al^{3+}$ solution (150 μL) in presence of $Fe^{3+}$ (150 μL) solution.

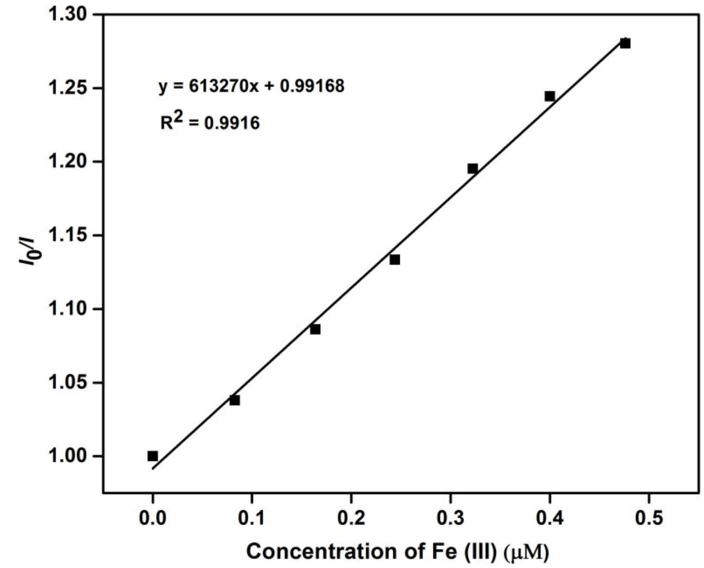

**Figure S49.** Stern-Volmer plot for the fluorescence quenching of **1′** upon addition of $Fe^{3+}$ solution.

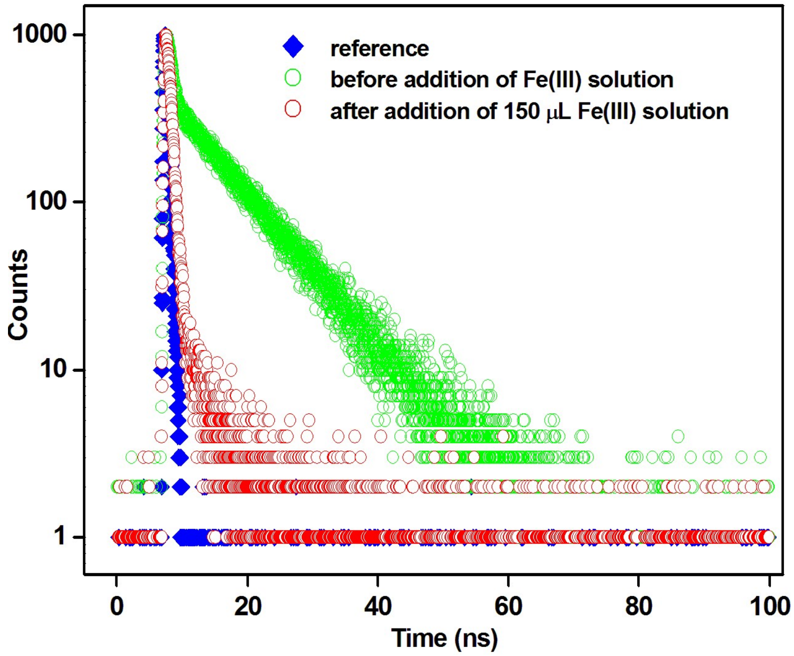

**Figure 50.** Lifetime decay profile of **1′** before and after addition of 150 μL of 2 mM $Fe^{3+}$ solution.

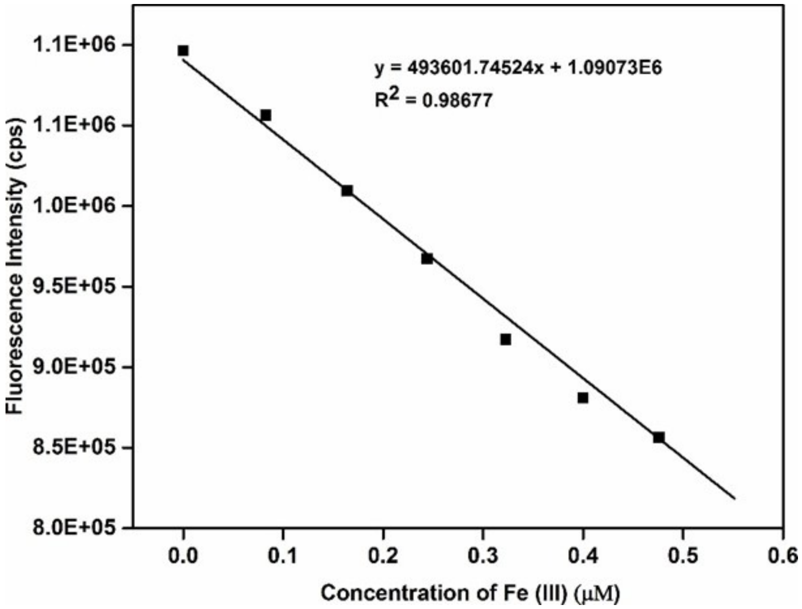

**Figure S51.** Change in the fluorescence intensity of **1′** in aqueous suspension as a function of $Fe^{3+}$ concentration.

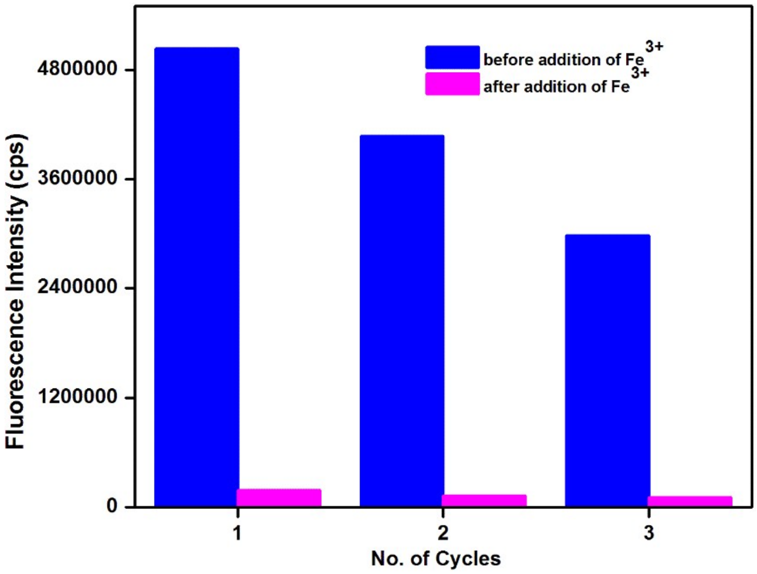

**Figure S52.** Reproducibility of the fluorescence quenching efficiency of the aqueous suspension of **1′** towards 2 mM $Fe^{3+}$ solution.

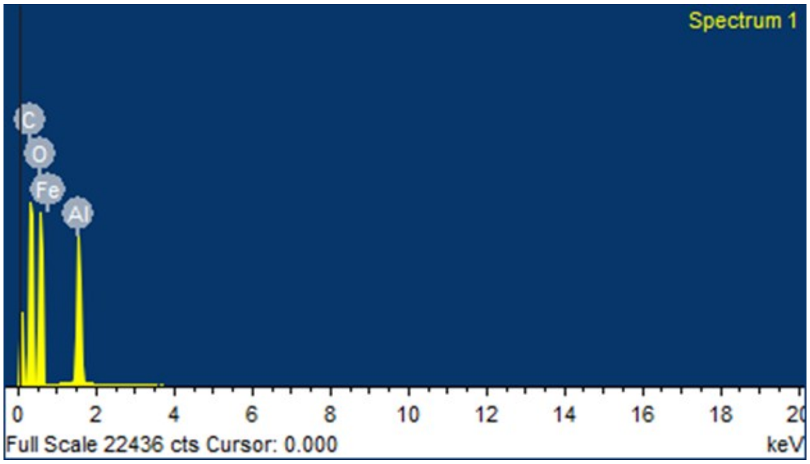

| Element | Weight% | Atomic% |
|---|---|---|
| C K | 41.35 | 50.69 |
| O K | 46.53 | 42.82 |
| Al K | 11.70 | 6.38 |
| Fe K | 0.42 | 0.11 |
| Total | 100.00 | 100.00 |

**Figure 53.** EDX spectrum of **1′** after treatment with 2 mM $Fe^{3+}$ aqueous solution.

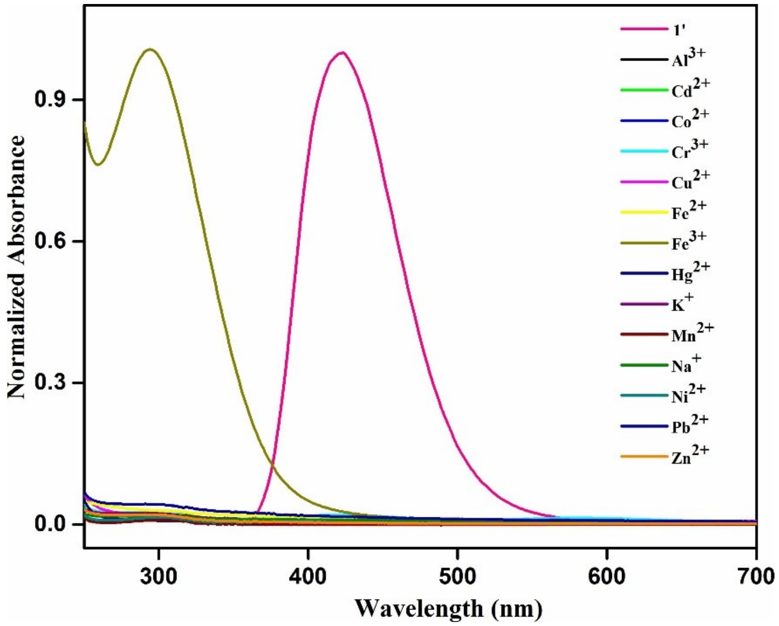

**Figure S54.** Spectral overlap between the absorption spectra of different metal ions and the emission spectra of **1′** in water.

**Table S1.** Micropore volumes (at $p/p_0 = 0.5$) of the Al-MIL-53-X compounds determined from $N_2$ adsorption isotherms.

| Sl. No. | Compound | Micropore volume ($cm^3 g^{-1}$) | Ref. |
|---|---|---|---|
| 1. | Al-MIL-53-$N_3$ | 0.34 | This Work |
| 2. | Al- MIL-53 | 0.54 | 1 |
| 3. | Al-MIL-53-Cl | 0.32 | 1 |
| 4. | Al-MIL-53-Br | 0.14 | 1 |
| 5. | Al-MIL-53-$CH_3$ | 0.32 | 1 |
| 6. | Al-MIL-53-$NO_2$ | 0.34 | 1 |
| 8. | Al-MIL-53-$(OH)_2$ | 0.04 | 1 |
| 9. | Al-MIL-53-$NH_2$ | 0.44 | 1 |
| 10. | Al-MIL-53-F | 0.48 | 2 |
| 11. | Al-MIL-53-$F_2$ | 0.16 | 3 |

**Table S2**. Comparison of the repose time, detection limit and analyte used for $H_2S$ detection for MOFs reported till date.

| Sl. No. | MOF | Response time (s) | Detection Limit | Medium Used | Analyte | Ref. |
|---|---|---|---|---|---|---|
| 1. | Al-MIL-53-$N_3$ | 180 | 90.47 nM | $H_2O$ | $Na_2S$ | This work |
| 2. | CAU-10-$N_3$ | 420 | 2.65 µM | HEPES buffer (10 mM, pH = 7.4) | $Na_2S$ | 4 |
| 3. | Ce-UiO-66-$N_3$ | 760 | 12.20 µM | HEPES buffer (10 mM , pH = 7.4) | NaSH | 5 |
| 4. | Ce-UiO-66-$NO_2$ | 760 | 34.84 µM | HEPES buffer (10 mM , pH = 7.4) | NaSH | 5 |
| 5. | Zr-DUT-52-$(NO_2)_2$ | 3300 | 20.00 µM | HEPES buffer (10 mM , pH = 7.4) | $Na_2S$ | 6 |
| 6. | Zr-UiO-66-$N_3$ | 180 | 118.00 µM | HEPES buffer (10 mM , pH = 7.4) | $Na_2S$ | 7 |
| 7. | Zr-UiO-66-$NO_2$ | ≈ 460 | 188.00 µM | HEPES buffer (10 mM , pH = 7.4) | $Na_2S$ | 8 |
| 8. | IRMOF-3-$N_3$ | < 120 | 28.30 µM | HEPES ethanol buffer (pH = 7.4) | NaSH | 9 |
| 9. | MN-ZIF-90 | - | - | PBS buffer (10 mM, pH = 7.4, 1% DMSO) | - | 10 |
| 10. | Al-TCPP-Cu | - | - | BBS buffer (20 mM, pH = 7.40) | - | 11 |
| 11. | Al-MIL-101-$N_3$ | - | 100 µM (UV-lamp | DMSO;<br>HBSS buffer | $Na_2S$ | 12 |

| | | | | | | |
|---|---|---|---|---|---|---|
| | | | excitation); 100 nm (laser excitation) | (pH = 8.2) | | |
| 12. | $Eu^{3+}/Cu^{2+}$@UiO-66-$(COOH)_2$ | 30 | 5.45 μM | Borate buffer (0.1 M, pH 8.5) | NaSH | 13 |
| 13. | $Tb^{3+}$@Cu-MOF | 120 | 1.20 μM | HEPES buffer (10 mM , pH = 7.4) | $Na_2S$ | 14 |

**Table S3.** Average excited-state lifetime (<$\tau$>) values of **1′** before and after addition of 100 μL of 0.21 (M) $Na_2S$ solution ($\lambda_{ex}$ = 308 nm).

| Volume of $Na_2S$ solution added (μL) | $B_1$ | $B_2$ | $a_1$ | $a_2$ | $\tau_1$ (ns) | $\tau_2$ (ns) | <$\tau$>* (ns) | $\chi^2$ |
|---|---|---|---|---|---|---|---|---|
| 0 | 0.0681 | 0.0091 | 0.415 | 0.585 | 0.702 | 7.429 | 4.637 | 1.020 |
| 100 | 0.0368 | 0.000 | 1.00 | 0.000 | 8.949 | 0.000 | 8.949 | 1.002 |

<$\tau$>* = $a_1 \tau_1 + a_2 \tau_2$

**Table S4.** A comparison of the Stern-Volmer constant ($K_{sv}$), detection limit and medium used for the sensing of $Fe^{3+}$ ion for MOFs reported till date.

| Sl. No. | MOF | $K_{sv}$ ($\times 10^4$ $M^{-1}$) | Detection Limit | Medium Used | Ref. |
|---|---|---|---|---|---|
| 1. | Al-MIL-53-$N_3$ | 61.32 | 0.03 μM | Water | This work |
| 2. | Al-MIL-53 | - | 0.90 μM | PBS Buffer | 15 |
| 3. | $[Zr_6O_4(OH)_4(2,7\text{-}CDC)_6]\cdot 19H_2O\cdot 2DMF$ | 0.55 | 0.91 μM | Water | 16 |
| 4. | $[La(TPT)(DMSO)_2]\cdot H_2O$ | 1.36 | - | Ethanol | 17 |
| 5. | $[H(H_2O)_8][DyZn_4(imdc)_4(im)_4]$ | 2.88 | - | DMSO | 18 |
| 6. | $EuL_3$ | 0.41 | 100.0 μM | Ethanol | 19 |
| 7. | $[Eu_2(MFDA)_2(HCOO)_2(H_2O)_6]\cdot H_2O$ | - | 0.33 μM | DMF | 20 |
| 8. | $[Cd(H_2L_a)_{0.5}(H_2L_b)_{0.5}(H_2O)]$ | - | 10.0 μM | Water | 21 |
| 9. | $[(CH_3)_2NH_2]\cdot[Tb(bptc)]\cdot x$solvents | - | 72.76 ppm | Ethanol | 22 |
| 10. | $[Ln_2(Ccbp)_3\cdot 6H_2O]\cdot 3Cl^-\cdot 4H_2O$ | 11.43 | - | Ethanol | 23 |
| 11. | $Eu^{3+}$@MIL-124 | 3.87 | 0.28 μM | Water | 24 |
| 11. | $[Ln(Hpzbc)_2(NO_3)]\cdot H_2O$ | - | 26.0 μM | Ethanol | 25 |

| | | | | | |
|---|---|---|---|---|---|
| 12. | $[\mathrm{Tb(BTB)(DMF)}]\cdot 1.5\mathrm{DMF}\cdot 2.5\mathrm{H_2O}$ | - | 10.0 μM | Ethanol | 25 |
| 13. | $[\mathrm{Tb_4(OH)_4(DSOA)_2(H_2O)_8}]\cdot(\mathrm{H_2O})_8$ | 3.5 | - | Water | 26 |
| 14. | $[\mathrm{Ba_5(ADDA)_5(EtOH)_2(H_2O)_3}]\cdot 5\mathrm{DMF}$ | - | 0.21 μM | Acetone | 27 |
| 15. | $\mathrm{Tb^{3+}@Cd\text{-}MOF}$ | 11.08 | 10.0 mM | DMF | 28 |

**Table S5.** Average excited state lifetime ($<\tau>$) values of **1′** before and after addition of 150 μL of 2 mM $\mathrm{Fe^{3+}}$ solution ($\lambda_{ex}$ = 308 nm).

| Volume of $\mathrm{Fe^{3+}}$ solution added (μL) | $B_1$ | $B_2$ | $a_1$ | $a_2$ | $\tau_1$ (ns) | $\tau_2$ (ns) | $<\tau>$* (ns) | $\chi^2$ |
|---|---|---|---|---|---|---|---|---|
| 0 | 0.0673 | 0.0145 | 0.183 | 0.817 | 0.443 | 9.222 | 7.62 | 0.997 |
| 150 | 0.0983 | 0.0010 | 0.919 | 0.806 | 0.437 | 3.699 | 3.38 | 0.960 |

* $<\tau> = a_1\tau_1 + a_2\tau_2$

## References

1. S. Biswas, T. Ahnfeldt and N. Stock, *Inorg. Chem.*, 2011, **50**, 9518–9526.
2. S. Biswas, T. Remy, S. Couck, D. Denysenko, G. Rampelberg, J. F. M. Denayer, D. Volkmer, C. Detavernier and P. V. D. Voort, *Phys. Chem. Chem. Phys.*, 2013, **15**, 3552-3561.
3. S. Biswas, S. Couck, D. Denysenko, A. Bhunia, J. F. M. Denayer, D. Volkmer, C. Janiak and P. V. D. Voort, *Microporous Mesoporous Mater.*, 2013, **181**, 175-181.
4. S. Nandi, H. Reinsch, S. Banesh, N. Stock, V. Trivedi and S. Biswas, *Dalton Trans.*, 2017, doi: 10.1039/C1037DT02293J.
5. A. Buragohain and S. Biswas, *CrystEngComm*, 2016, **18**, 4374–4381.
6. R. Dalapati, S. N. Balaji, V. Trivedi, L. Khamari and S. Biswas, *Sens. Actuators, B*, 2017, **245** 1039–1049.
7. S. S. Nagarkar, T. Saha, A. V. Desai, P. Talukdar and S. K. Ghosh, *Sci. Rep.*, 2014, **4**, 7053-7058.
8. S. S. Nagarkar, A. V. Desai and S. K. Ghosh, *Chem. Eur. J.* , 2015, **21**, 9994–9997.
9. X. Zhang, J. Zhang, Q. Hu, Y. Cui, Y. Yang and G. Qian, *Appl. Surf. Sci.*, 2015, **355**, 814-819.
10. H. Li, X. Feng, Y. Guo, D. Chen, R. Li, X. Ren, X. Jiang, Y. Dong and B. Wang, *Sci. Rep.*, 2014, **4**, 4366-4370.
11. Y. Ma, H. Su, X. Kuang, X. Li, T. Zhang and B. Tang, *Anal. Chem.*, 2014, **86**, 11459-11463.
12. A. Legrand, A. Pastushenko, V. Lysenko, A. Geloen, E. A. Quadrelli, J. Canivet and D. Farrusseng, *ChemNanoMat*, 2016, **2**, 866 – 872.
13. X. Zhang, Q. Hu, T. Xia, J. Zhang, Y. Yang, Y. Cui, B. Chen and G. Qian, *ACS Appl. Mater. Interfaces*, 2016, **8**, 32259-32265.

14. X. Zheng, R. Fan, Y. Song, A. Wang, K. Xing, X. Du, P. Wang and Y. Yang, *J. Mater. Chem. C*, 2017, **5**, 9943-9951.
15. C.-X. Yang, H.-B. Ren and X.-P. Yan, *Anal. Chem.* , 2013, **85**, 7441−7446.
16. A. Das and S. Biswas, *Sens. Actuators, B*, 2017, **250**, 121–131.
17. C. Zhang, Y. Yan, Q. Pan, L. Sun, H. He, Y. Liu, Z. Liang and J. Li, *Dalton Trans.*, 2015, **44**, 13340-13346.
18. Y.-F. Li, D. Wang, Z. Liao, Y. Kang, W.-H. Ding, X.-J. Zheng and L.-P. Jin, *J. Mater. Chem. C*, 2016, **4**, 4211-4217.
19. M. Zheng, H. Tan, Z. Xie, L. Zhang, X. Jing and Z. Sun, *ACS Appl. Mater. Interfaces*, 2013, **5**, 1078-1083.
20. X.-H. Zhou, L. Li, H.-H. Li, A. Li, T. Yang and W. Huang, *Dalton Trans.*, 2013, **42** 12403-12409.
21. Y. Wu, G.-P. Yang, Y. Zhang, N. Shi, J. Han and Y.-Y. Wang, *RSC Adv.*, 2015, **5**, 90772-90777.
22. X.-L. Zhao, D. Tian, Q. Gao, H.-W. Sun, J. Xu and X.-H. Bu, *Dalton Trans.*, 2016, **45**, 1040-1046.
23. K.-M. Wang, L. Du, Y.-L. Ma, J.-S. Zhao, Q. Wang, T. Yan and Q.-H. Zhao, *CrystEngComm*, 2016, **18**, 2690-2700.
24. X.-Y. Xu and B. Yan, *ACS Appl. Mater. Interfaces*, 2014, **7**, 721-729.
25. C.-X. Yang, H.-B. Ren and X.-P. Yan, *Anal. Chem.*, 2013, **85**, 7441-7446.
26. X.-Y. Dong, R. Wang, J.-Z. Wang, S.-Q. Zang and T. C. Mak, *J. Mater. Chem. A*, 2015, **3**, 641-647.
27. R. Wang, X. Liu, A. Huang, W. Wang, Z. Xiao, L. Zhang, F. Dai and D. Sun, *Inorg. Chem.*, 2016, **55**, 1782–1787.
28. H. Weng and B. Yan, *Sens. Actuator B, Chem.*, 2016, **228**, 702-708.